2022

EXPERIMENTAL ANALYSIS AND COMPUTER SIMULATION OF A LABORATORY-SCALE INTERMITTENT WATER SUPPLY SYSTEM

Brian Rivers
Michigan Technological University, bwrivers@mtu.edu

EXPERIMENTAL ANALYSIS AND COMPUTER SIMULATION OF A LABORATORY-SCALE INTERMITTENT WATER SUPPLY SYSTEM

By

Brian W. Rivers

A REPORT

Submitted in partial fulfillment of the requirements for the degree of

MASTER OF SCIENCE

In Environmental Engineering

MICHIGAN TECHNOLOGICAL UNIVERSITY

2022

This report has been approved in partial fulfillment of the requirements for the Degree of MASTER OF SCIENCE in Environmental Engineering.

Department of Civil, Environmental, and Geospatial Engineering

Report Advisor:	*David W. Watkins*
Committee Member:	*Brian D. Barkdoll*
Committee Member:	*Veronica L. Webster*
Department Chair:	*Audra Morse*

TABLE OF CONTENTS

Acknowledgements

First and foremost, I would like to acknowledge the life of abundance my family has provided: in love, support, education, and countless other resources, all of which stems from my parents, Donald and Lori Rivers. For almost thirty years, their innumerable sacrifices of time, effort, tears, and money, wove the strongest safety net I could ask for. The happy, secure, and successful futures my brothers and I build are a direct product of the constant work Mom and Dad perform on behalf of this family. Compounding these gifts are those from my grandparents: Bill and Louis Buehler, and Barbara and Reinhardt Rivers; if not for their sacrifices on the ridgeline dairy farms of southeastern Minnesota, the privileges, achievements, and camaraderie my brothers, cousins, and myself enjoy would have been substantially more difficult, if not impossible to attain.

Next, I would like to thank my Advisor, Dr. David Watkins, and committee members Dr. Brian Barkdoll and Dr. Veronica Webster for dedicating their focus to this report and sharing their respective expertise to strengthen it. I have enjoyed all of their classes immensely and am proud to submit this report for their approval.

I would be remiss to omit the enthusiastic and tireless assistance from Lab Technician Robert Fritz, whose guidance and skill in the trades were crucial not simply in the construction of the IWS but for its inventive material sourcing and relatively low cost. Environmental engineering doctoral candidate Kenny Larsen also made a significant contribution to this project by lending me digital cameras to record the demand node outflows. Finally, I'd like to thank Tom Polkinghorn, the Dow Building Manager for promptly responding to drainage issues in Lab 105 and 106 that may have saved weeks of delays.

Many members of Houghton, Hancock, and the greater Keweenaw deserve credit for helping me settle into this community. Namely, the outpouring of generosity, friendship, and food from my roommates Christian Sheja and Hunter King and have made the pursuit of this degree much more enjoyable, comfortable, and fulfilling than had we not shared a kitchen. Bailey Papes also deserves recognition for keeping me informed about the details of report-writing and being an excellent office partner.

Finally, I'd like to dedicate this report to the people of Lucma District in La Libertad, Peru. Throughout the 21 months I spent among the district's communities, myriad obstacles to obtaining clean, reliable, and abundant drinking water, among other basic human necessities, struck me as distressing. Yet, the love, friendship, and heaps of food they extended to me demonstrated their resilience in the face of such adversity and catalyzed this pursuit of IWS research.

Beyond internal interest, the MTU research team hopes the results of this study will inform the findings of ongoing research into intermittent water systems undertaken by a team at the University of Exeter in Exeter, United Kingdom.

Abstract

Intermittent water systems (IWS) are prevalent throughout developing regions of the world. However, few tools exist to predict IWS performance because modeling transient flow is difficult: IWS networks can experience widely fluctuating conditions, ranging from completely empty to completely full (pressurized flow). An experimental IWS, consisting of a 50.75-gallon reservoir, an elevated distribution network, and four outlets was constructed to study the hydraulics of IWS. Three experiments were run on the system that represented two falling-head scenarios and a constant-head scenario. Computer simulation models of the experimental IWS were developed in EPANET 2.2.0 and EPA-SWMM 5.1, which are open-source modeling software for pressured water distribution networks and stormwater conveyance systems, respectively. EPANET 2.2.0 was incapable of representing flows observed in the experiments, likely due to the steady-state assumptions inherent to its global gradient algorithm. However, EPA-SWMM 5.1, which models the propagation of network flows with dynamic wave routing, was able to generate outflow hydrographs that emulated experimental discharge flows. Therefore, it is recommended that further verification be undertaken to validate SWMM's capacity to model IWS systems under a range of hydraulic scenarios. If SWMM can withstand rigorous experimentation, potential may exist for this software to be retooled for the design of IWS.

Introduction

Background and Motivation

In many industrialized and high-income regions of the world, municipal drinking water systems are complex networks of infrastructure that include pipes, reservoirs, treatment plants, and pumps, to name a few of myriad components. If the system collects, treats, and delivers constant water to users, these systems are known as continuous water systems (CWS). Ideally, CWS provide water to their consumers at a consistent pressure and quality. However, these systems are distinguished by drinking water's availability throughout the day and night.

If service is available to users for any period less than 24 hours per day, the system is known as an intermittent water system (IWS). Typically, IWS include much of the same infrastructure as CWS and, if properly constructed, operated, and maintained, can also supply drinking water at a consistent pressure and quality. However, the primary difference between CWS and IWS is the availability of service. As indicated by the name, IWS do not provide their users with continuous water supply, and instead, water may only be available at scheduled or even unpredictable intervals. Service may be apportioned between districts, or service to all districts may be shut off at times to allow reservoirs to fill (Campisano et al., 2018).

For reasons related to health, administration, lifecycle performance, and social welfare, an IWS is less desirable than a CWS. However, considerations such as cost, water scarcity, high demand, and utility management may dictate the rationing of flows throughout the system. For these reasons and others, many water distribution systems in developing regions of the world operate intermittently to apportion water among their users or conform to local resource constraints. In 2016, as many as 300 million people throughout the world received water via IWS. Considering the intensifying burden placed on water resources, global phenomena such as rapid urbanization, enhanced standards of living, and climate change will likely increase this estimate (Kumpel and Nelson, 2016).

While intermittent operation of water supply may affect the availability of service, cycling periods of flow throughout the system may have significant implications for water quality. During normal operation of an IWS, the pipes of the distribution network may transition between flowing completely full, partially full, and completely empty. When water is released into a vacant distribution system from a reservoir, the water may encounter entrapped air as the pipes fill. When the system transitions from a pressurized to an unpressurized state (e.g., if disconnected from the supply), pipes may vacate, and if the pressure becomes negative, a siphon can be created at existing leaks or faulty pipe connections. As discussed in Kumpel and Nelson (2016), air, water, and soil from around the pipe may be drawn into the system, introducing contaminants that can be transported to points of use. Furthermore, continued cycling of pressures, air, and water may also harbor microbial growth on the interior surface of the pipes which can serve as a source of contamination downstream of any centralized water treatment. Cycling of pressures can also affect the durability of the system.

Truncated service can also deny system users the opportunity to meet the basic access level, defined as 20 LPCD by the World Health Organization, or intermediate access, defined as 50 LPCD by Howard and Bartram (2003). This daily demand incorporates water for drinking, cooking, washing, or other consumptive, domestic activities. Furthermore, this demand threshold also incorporates water used for sanitary purposes. Inadequate or inequitable service may force consumers to forego hygienic behaviors throughout the day, such as washing hands, flushing toilets, or bathing (Mihelcic et al, 2009).

As a result of inconsistent service, many communities with IWS find it necessary to adapt their water collection behaviors to maximize the daily quantity of water available to them. Because water is not available at times convenient to users, intermittent service may even entice users to find less reliable and more vulnerable sources of water that require travel and transport (Mihelcic et al., 2009).

For some users, adaptation to IWS may involve routing tap water to a domestic storage tank, filling the tank when supply is available, and using the water in the tank after the flow from the IWS ceases. Filling the tank may involve leaving water taps open constantly or for a long period of time. Domestic tanks have the distinct advantage of alleviating scarcity for short periods and may allow users to treat large batches of water effectively at the point of use. However, domestic storage devices like tanks may also invite contamination vectors if they are left uncleaned or unprotected (McKenzie, 2011; Dubasik, 2017). For others in low-income communities who may not have financial or logistical means to store water in a domestic tank, collection behavior may involve diverting tap water into various unprotected bins, buckets, or other storage devices for later use. In communities where the timing of IWS service is not scheduled, some households may leave domestic taps open to indicate when the water service has returned (Cabrera-Béjar and Tzatchkov, 2012). Beyond storage, drinking water at open taps may also be illegally diverted to crops or livestock, often regarded as a misuse or waste of drinking water (McKenzie, 2011).

While waste itself is regrettable, scarcity-driven behaviors such as water hoarding may beget other complications such as lower pressure and limited access throughout the system. Dubasik (2017) found that scarcity-driven behaviors enacted at lower elevations in an IWS caused inequitable service for users at higher elevations and caused degradation of the system. McKenzie (2011) found that these same behaviors enacted at higher elevations, but closer to a main line, caused user inequity further downstream in an IWS. If users are not informed of the consequences of hoarding water or persuaded to adapt their collection behaviors, communal access to drinking water in an IWS may suffer.

Additionally, waste of water resources may beget waste in human resources. Distribution equity is salient in many rural and low-income communities because inconsistent service requires increased effort by impoverished consumers to acquire water, a basic necessity of life and a human right (UN, 2014). Enforcement of water regulations may depend on the presence of water meters or the inclination of the local government, both of which can be absent in rural or

low-income communities. Thus, local authorities, volunteer committees, or individual citizens are burdened with keeping neighbors from using more than their share. Furthermore, households that delegate collection responsibilities among their members force them to sacrifice time, energy, or educational and economic opportunities that are already scarce in developing communities.

Low-income, rural, and developing communities may lack resources to employ professional design, construction, and management services. Thus, the design of a distribution system may be driven by the preference of local authorities, the abilities of local laborers, availability of materials, or limited financial resources. As a result, designs could neglect existing environmental and topographical conditions, fluctuations in demand, equitable access, and community growth. Beyond initial construction, planning for future maintenance and monitoring activities and their associated budgetary allocations can also vary between systems. Neglect of comprehensive, lifecycle planning can relegate distribution systems to intermittent operation and leave the infrastructure vulnerable, water service unreliable, and the users underserved.

Modeling Challenges and Approaches

While many modern software tools exist to simulate water distribution systems, most, if not all, fail to appropriately model IWS operation. For example, EPANET 2.2.0, a widely used software package for extended-period simulation of hydraulic and water quality conditions in distribution systems, may only model CWS. EPANET 2.2.0 integrates a global gradient algorithm to perform pressure-driven and demand-driven analyses that satisfy conservation of mass (continuity equations) and conservation of energy. However, this process, known as hydraulically balancing the network, assumes that pipes are always flowing full and does not account for transient flow conditions, which are observed in many IWS (Rossman et al. 2020).

Other modeling programs, like NeatWork, are oriented for work in developing communities but also assume steady-state flow or CWS operation. Neatwork, developed by the non-governmental organization Agua Para La Vida, is a program driven by the modeling of intermittent demands, assuming that withdrawals from points-of-use, or faucets, are random. This can be thought of as intermittent (or stochastic) demand modeling, as opposed to intermittent supply modeling explored in this paper. The program incorporates a heuristic approach for modeling demand-dependent analysis in gravity-fed water systems, while considering random configurations of open and closed faucets. NeatWork omits mechanical infrastructure such as pumps to simplify operation and find the lowest-cost solution (Babonneau et al., 2019).

Transient flow conditions, such as pipes transitioning between empty and full, can be modeled in programs that are not necessarily designed for drinking water distribution systems, such as the United States Environmental Protection Agency’s (EPA) Storm Water Management Model (SWMM). This paper investigates the repurposing of SWMM Version 5.1.015, released on July 20th, 2020, for IWS modeling. In SWMM, water distribution pipes can be approximated for partially full flow under non-steady-state flow conditions. SWMM employs dynamic wave routing

that can simultaneously solve continuity, energy, and momentum equations throughout the system (Rossman, 2017). Therefore, by modifying the model settings and input parameters, the program, originally developed for stormwater hydraulics, can more accurately describe IWS operation than models designed for CWS. SWMM's appropriateness in modeling IWS has been investigated by Campisano et al. (2018), who tested SWMM against experimental field data and a traditional modeling approach based on the theory of the rigid water column. Dubasik (2017) found that despite difficulty in calibrating SWMM, the program was effective in modeling IWS conditions for a rural distribution system in Panama. Furthermore, analysis revealed that the program could provide potential allocation solutions for users at higher elevations of an IWS.

Study objectives

This study aims to identify gaps in the IWS knowledge base by detailing IWS performance under varying hydraulic conditions. By comparing the observations with model outputs from SWMM 5.1.015 and EPANET 2.2.0, this study will also investigate the applicability of each program to gravity-driven flow in IWS, under falling head and constant head scenarios in a reservoir. The following sections detail the steps taken to meet these objectives. The Methods section explains the parameters of the laboratory-scale IWS, as well as the procedures followed in the three experiments. Parameters and assumptions applied in the assembly of the EPANET 2.2.0 and EPA-SWMM 5.1 models are also explained in the Methods section. Next, the results of the lab experiments and computer simulations are examined, compared, and discussed. Finally, the report will summarize the findings of this study and point to future work.

Methods

Laboratory layout

Throughout the summer and autumn of 2021, an experimental IWS system was constructed on a six-meter by five-meter footprint inside a laboratory of the Dow Environmental Sciences and Engineering Building at Michigan Technological University in Houghton, Michigan. The model IWS system consisted of a 192-liter (50.75-gallon) reservoir, an elevated distribution network consisting of polyvinyl chloride (PVC) pipes, a control valve at the reservoir, and four discharge ("demand" flow) nodes, three water collection bins, and one drainage trough (Figures 1-3).

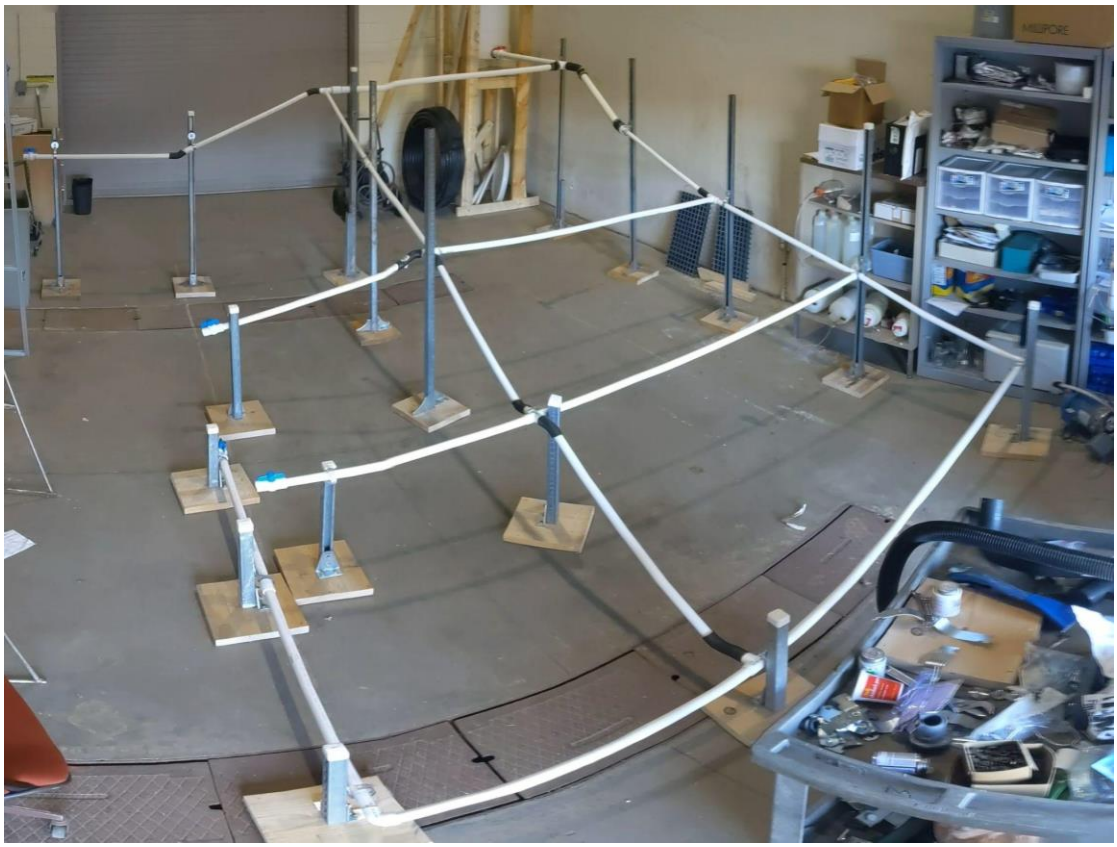

Figure 1. Panoramic of experimental IWS in the Dow Environmental Engineering and Sciences building at Michigan Technological University.

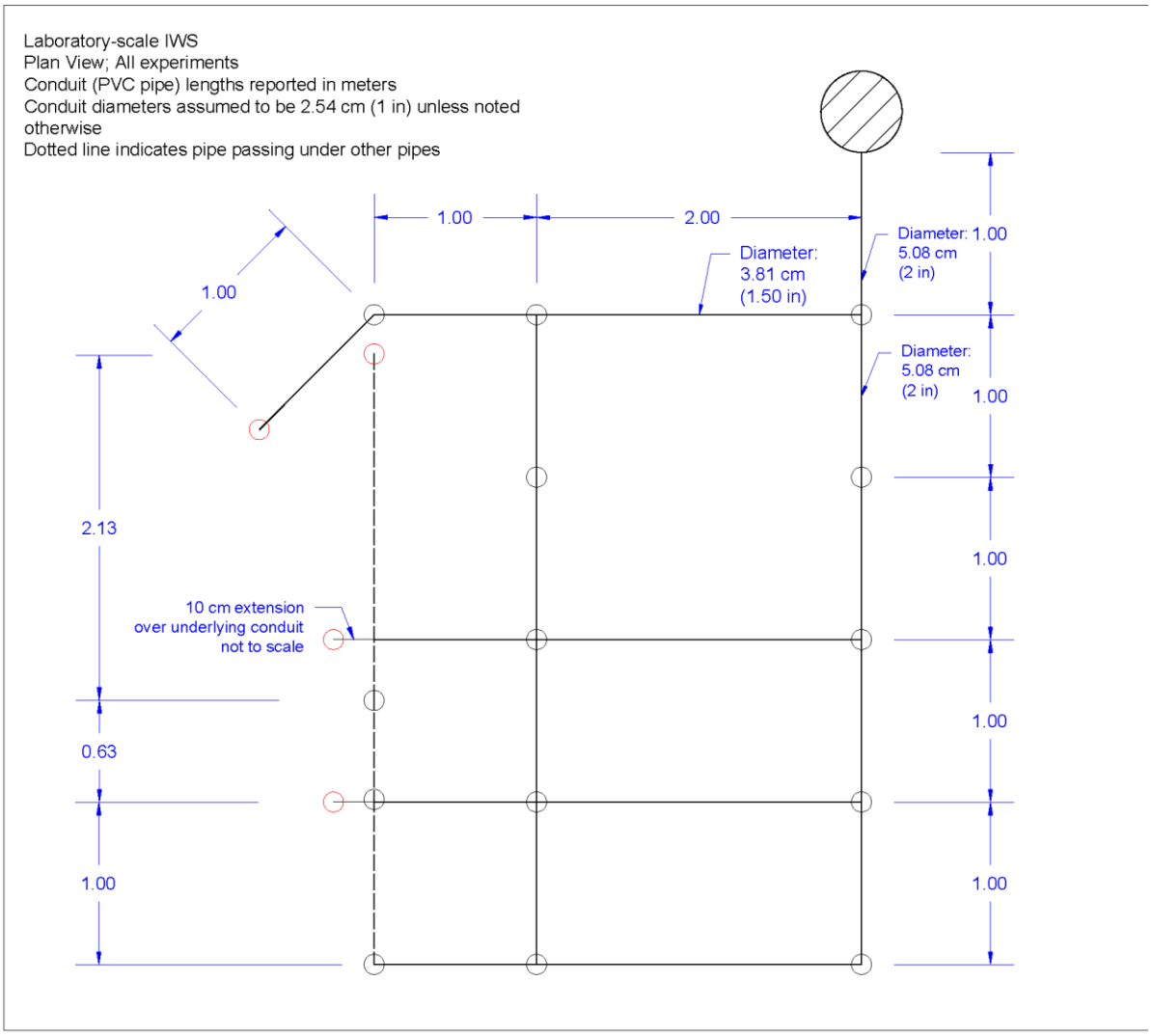

Figure 2. Plan-view schematic of IWS system

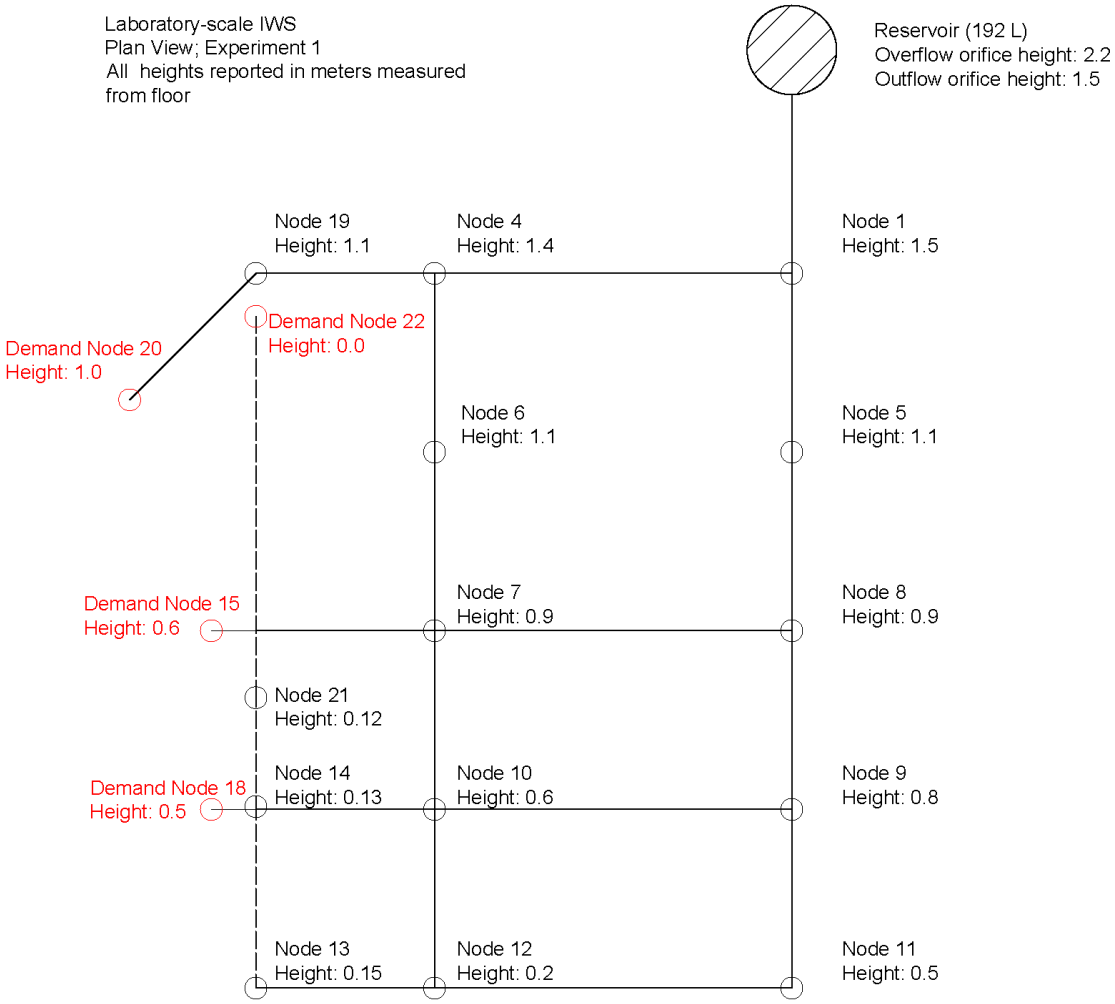

Figure 3. Experiment 1 node heights in the laboratory-scale IWS. Dotted lines represent pipe sections laid underneath other pipe sections. A node height map for experiments 2 and 3 is seen in Figure 1a (Appendix).

The reservoir (Figures 4 and 5) consisted of a modified 192-liter (50.75-gallon) translucent, uncapped plastic barrel with two orifices; a controlled 50.8-mm (2-inch) outflow orifice whose invert was located 40 mm above the bottom surface of the barrel, and a 10-mm overflow orifice located 700 mm above the barrel's bottom. A 10-mm garden hose was connected to the overflow orifice to ensure a consistent head at the beginning of each trial. Excess water was diverted into a section of the drainage trough downstream of another section partitioned for discharge measurement. The outflow orifice was equipped with a 50.8-mm (2-inch)-diameter ball valve that regulated flow into the distribution network. Five-gallon (18.9-L) increments were marked on the outer surface of the barrel to gauge change in water level over time. The height of each 5-gallon increment was calculated from measurement of the barrel's diameter. The level of the overflow was also marked on the outer surface of the barrel.

Figure 4. Reservoir barrel with tape marking 5-gallon increments

Figure 5. Reservoir platform

A wooden platform was constructed from plywood and two-inch by four-inch lumber to elevate the reservoir above the floor (Figure 5). For experiment 1, the platform was elevated to a height of 1.46 meters (4.79 feet) to ensure the invert of the outflow pipe was at a height of 1.50 meters (4.92 feet) and the maximum head, or water level at the overflow orifice, was approximately 2.20 meters (7.22 feet). For experiments 2 and 3, the platform was lowered to a height of 0.96 meters (3.15 feet) to ensure the invert of the outflow pipe was at a height of 1.00 meters (3.28 feet) and the maximum head was approximately 1.70 meters (5.58 feet).

The distribution network consisted of 21 PVC pipes with two sections with 50.8-mm (2-inch)-diameter pipes, a single 38.1-mm (1.5-inch)-diameter section, and eighteen sections of 25.4-mm (1-inch)-diameter pipes. The network was organized in a rectangular grid containing three

loops. Each junction or intersection of pipes constituted a “node,” totaling 14 conveyance nodes that connected two, three, or four sections of pipe. At nodes where changes in pipe diameter occur, adaptors were installed immediately upstream or downstream of the fitting. Stark differences in height between adjacent nodes necessitated the installation of flexible rubber conduit, modified from commercial automobile radiator hose (Figure 6). All nodes were elevated to a particular height; accompanying stands were constructed from Unistrut© PS1000HS metal framing to maintain a node’s specified height above the floor (Figure 7). Nodes where the water discharged from the network were referred to as “demand” nodes, referenced subsequently in this text as nodes 15, 18, 20, and 22 (see Figure 3). Each demand node was fitted with a 1-inch PVC ball valve that simulated an open tap. A 22.5-degree elbow, connected to a short length of 1-inch PVC, directed discharge into collection bins as seen in Figures 7 and 8. No stands were utilized for nodes 14, 21, and 22 because their height above the floor did not warrant a stand or because water discharged at the level of the floor.

Figure 6. Flexible rubber joint placed downstream of Node 4.

Figure 7. Demand Node 20 and its corresponding stand

Measurement of discharge volume at demand nodes 15, 18 and 20 was performed with translucent plastic 99.4-liter (26.3-gallon) storage bins, as shown in Figure 8. One-gallon (3.78-liter) increments were annotated in permanent marker on the bin’s outer wall. To account for the slope of the laboratory floor, the bins’ gallon increments were measured and marked in the

precise location of the bins during the experiments. Single gallons of water were poured into the bins and the water level of each gallon increment was noted in ascending order on the outer surface of the bin. Tape markings on the floor ensured that the bins were aligned properly in each trial. The lowest node, 22, was designed to discharge at the level of the floor into a 1.83-meter (6.00-foot) section of a laboratory drainage trough, which was modified at the upstream and downstream ends with Styrofoam “gates” to capture and measure node 22’s discharge volume. Water level heights were measured from the trough floor and were annotated on the lower Styrofoam gate (Figure 9). A hole, sealed with plumbers’ putty, was drilled through the lower gate to drain water at the end of each trial.

In each trial, video equipment was utilized to record the discharge filling each collection device as well as the time at which discharge began and ceased at each demand node. Three commercial digital cameras and a cell phone were placed on a tripod or nearby ledges to record flows at the four demand nodes. To extract the discharge hydrograph from each demand node, the video recording of the outflow was analyzed to determine the duration of flow between each gallon (3.78-liter) increment in the collection bin. Finally, a second cell phone camera was placed in front of the translucent reservoir to capture the water stage over the trial duration.

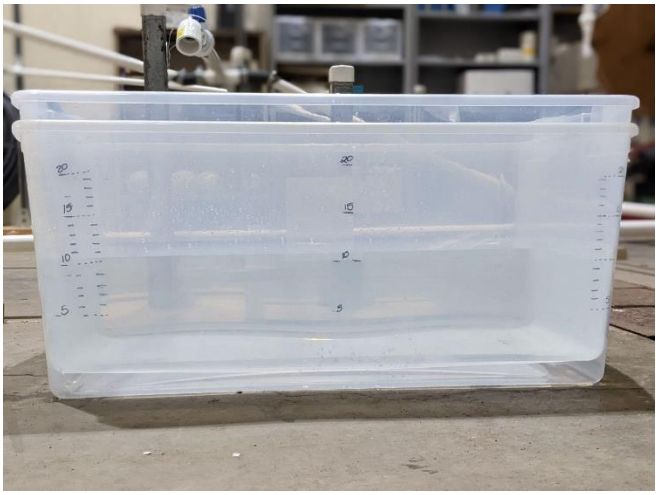

Figure 8. Collection bins. Bins were double-stacked in Trial 1, subsequent trials discharged into a single bin.

Figure 9. Downstream gate of the trough, annotated with quarter-inch measurements

Experimental Procedure

Three experiments were conducted on the laboratory IWS system. The first experiment examined a falling-head scenario with a 192.11-liter (50.75-gallon) reservoir supply, an initial head of 2.20 meters (7.22 feet) and an outlet height of 1.50 meters (4.92 feet). The second experiment again examined a falling-head scenario with an equal supply; however, the reservoir’s outlet was lowered to 1.00 meters (3.28 feet). Furthermore, all nodal heights greater than 1.00 meters were lowered to 1.00 meters in experiment 2. Finally, the third experiment was performed with the same reservoir and distribution system characteristics as experiment 2 but

maintained a constant head of water (1.70 meters, 5.58 feet) in the reservoir throughout each trial.

At least three trials were performed in each experiment. Before the trials in experiments 1 and 2 began, the reservoir was filled to the overflow orifice with municipal drinking water. Video recording of the experiment was then initiated at all five camera locations and a researcher announced the date, time, and trial number. The research then announced the opening of the reservoir outflow valve, thus initiating the trial. Recording of the trial continued at all locations until the flow decreased to an insignificant rate at each demand node. The researcher then announced the closing of the reservoir outflow valve and recording was terminated. The researcher then measured the volume of discharge collected in each of the bins and the drainage trough. After all discharge volumes were recorded, the collection bins were emptied, and water was either discharged in the drainage trough downstream of the gate or manually recycled into the reservoir with buckets.

In the third experiment, the reservoir was filled with 45 gallons of water before each trial. All video recorders were then initiated, and the researcher announced the date, time, and trial number. Then, the municipal spigot was opened two full rotations to achieve an inflow of approximately 0.61 LPS into the barrel through a hose. The researcher measured the time for the water level to increase from the 45-gallon mark to the 50-gallon mark, obtaining an inflow rate measurement. Once the water level reached the overflow orifice, the reservoir's outflow valve was opened to an angle calibrated to match the measured inflow, thus beginning the trial. The reservoir's outflow valve was left at this partially open setting for the duration (approximately 260 seconds) of the trial, after which the valve was shut.

Later, researchers examined the video recording of the demand nodes for each experiment to identify the precise timing and duration of each node's flow. The duration of flow at each node was then combined with the volume measured in the corresponding bin or trough to determine the average flow rate at the demand node. The videos of the demand nodes were also examined to create outflow hydrographs. By measuring the filling time between gallon (3.78-liter) increments marked on the collection bins, time-varying flow rates could be estimated.

Computer Simulations

Two computer simulation models of the laboratory IWS were assembled to represent experimental flows under continuous and intermittent supply conditions. First, a model to approximate continuous flow was constructed in the program EPANET 2.2.0 and was calibrated to simulate flow under the physical, temporal, and hydraulic parameters of the experimental IWS. Hydraulic components available in the software such as tanks, links, and junctions represented the barrel, PVC pipes, and fittings of the experimental set-up, respectively. The layout of these devices in EPANET reflected the layout of the experimental schematic, as seen in Figure 10. The properties of each model component mimicked the as-built properties of the experimental IWS, such as the elevation of each node, the diameter and volume of the barrel, and the initial water level in the barrel.

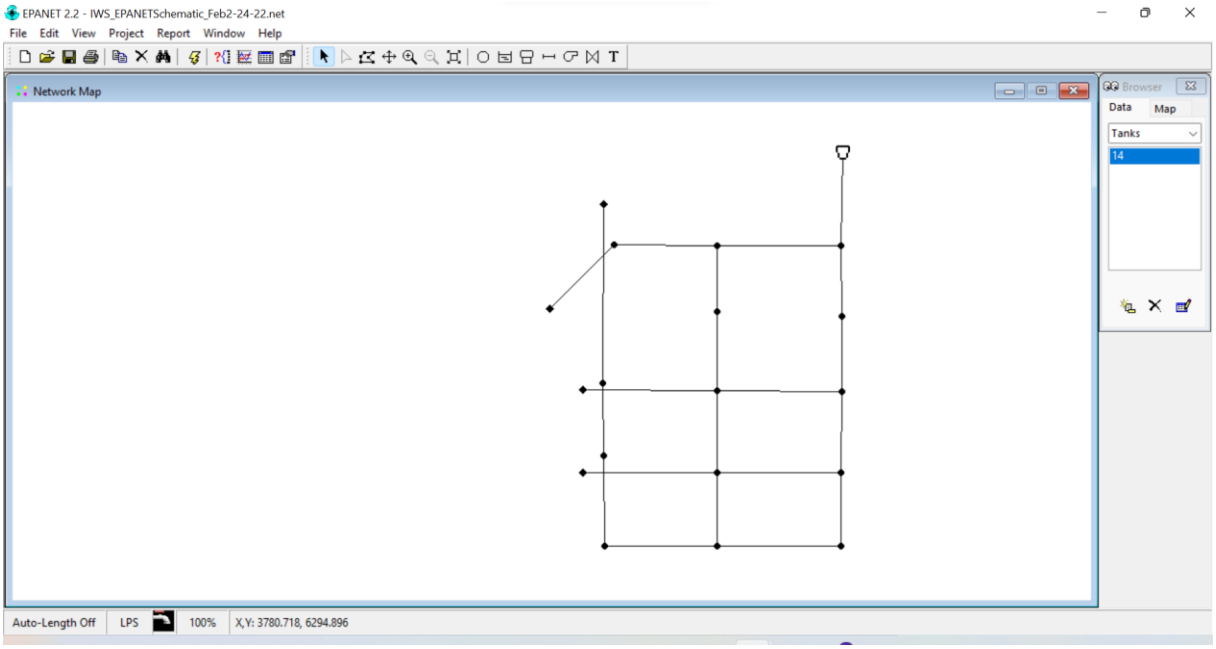

Figure 10. Schematic of IWS system in EPANET 2.2.0

Once the component properties and system layout were established, operating parameters of the system were applied to hydraulic analysis parameters (Table 1). Time-step patterns were established to represent the stage-inflow relationship between the tank and the distribution network. Short simulations, or time steps, were identified to mimic the short duration of the experiments. For example, the total duration of each falling-head experiment was approximately three minutes, with appreciable outflow from the reservoir barrel occurring for only one minute. Thus, the duration of the EPANET simulations was three minutes and each hydraulic time step was set to the minimum length of one minute.

Table 1. EPANET analysis parameters used for simulation

Time Property	Hrs:Min	Hydraulic Property	Value
Total Duration	0:03	Flow Units	LPS
Hydraulic Time Step	0:01	Headloss formula	Chezy-Manning
Pattern Time Step	0:01	Emitter Exponent	0.5
Reporting Time Step	0:01	Demand Model	DDA

At each demand node, emitter coefficients which describe discharge (flow) per unit of pressure drop, were calibrated. It was hypothesized that researchers could fine-tune EPANET's modeled discharge to match the experimental discharge by adjusting the coefficients. A wide range of coefficients were tested at each node in the simulation of experiment 1. Eventually, smaller coefficients, ranging between 0 and 2, as seen below in Table 2 were found to produce positive discharge (demand) patterns at three of the four nodes.

Table 2. Emitter coefficients; combinations producing 3 positive demands and 1 negative demand (usually node 22).

Demand Node	22	20	15	18
Emitter Coefficient	0.5	2.00	2.00	0.5
	0.5	1.00	1.25	0.5
	0.5	1.00	1.00	0.5
	0.5	1.00	1.25	0.5

Similar to the EPANET 2.2.0 model, three models representing the experiments were constructed in EPA-Storm Water Management Model (SWMM). The tank, nodes, and pipes of the EPANET 2.2.0 model were substituted for a storage unit, network junctions, and links, with the addition of an outfall at each demand node in SWMM. In experiment 3, the storage unit, representing the reservoir barrel, was changed to a fixed outfall to simulate constant-head conditions. Again, component properties and the system's overall layout were organized to replicate the laboratory-scale, experimental IWS (Figure 11). As-built properties like elevation, pipe diameter, and initial pressure head in the storage unit were modeled by individually specifying each component's properties within the program.

Hydraulic parameters were estimated and applied to the system. A tabular storage curve detailed a stage-surface area relationship within the storage unit to approximate the barrel's volume (See Table 1a, Appendix). All conduits were assigned a Manning's roughness coefficient of n = 0.009 (EngineeringToolbox, 2004a). At all network nodes (not demand nodes), a surcharge depth of 200 meters (656 feet) was identified to prevent SWMM from spilling flow (Campisano et al. 2018).

Designation of conduit entry and exit loss coefficients was based on the sizes and types of junctions connected at the upstream and downstream ends of the pipe (Table 2a, Table 3). For example, conduit 1, connected to the storage unit, was assigned an entry coefficient of k = 0.05 to simulate the completely open, 2-inch ball valve applied in experiments 1 and 2. However, in experiment 3's simulation, conduit 1 was assigned an entry loss coefficient of k = 200 to account for the ball valve being partially closed, approximately ⅔ of a full quarter rotation (Engineering ToolBox, 2004b) All other conduits' entry and exit coefficients were reported as friction loss equivalent lengths in meters to account for varying pipe diameters and flow direction (Engineering ToolBox, 2004c). With the exception of conduit 1, loss coefficients remained constant across each model because network junctions were not altered in the experiments.

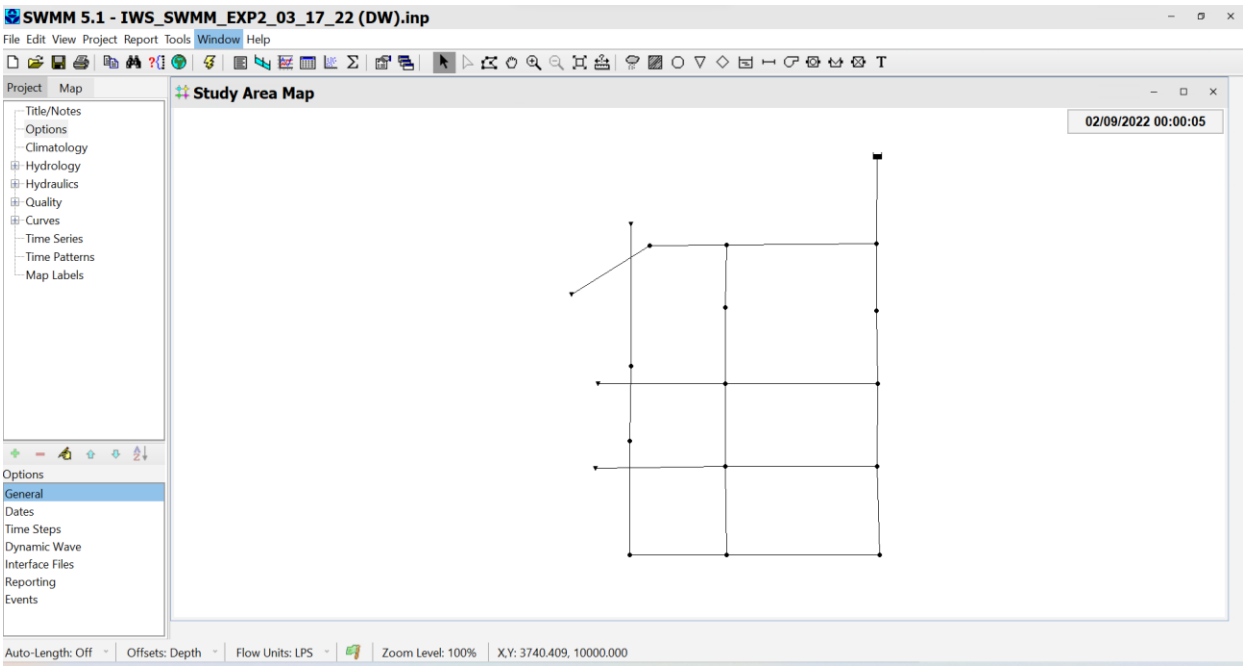

Figure 11. Screenshot of EPA-SWMM model for experiment. The storage unit and the connected "conduit 1" are seen at the top of the distribution system layout.

Table 3. Entry/ Exit loss coefficients used in EPA-SWMM network

Minor Loss Coefficient	Description	Friction Loss Equivalent Length (m)	Description
k = 0.05 k = 200	Ball valve, Fully open Ball valve, ⅔ closed	1.620	90-deg elbow, standard sharp inside radius, 1"
k = 0.04	1-in PVC coupler	2.440	Tee Flow-Branch, 1.5"
Friction Loss Equivalent Length (m)		0.427	45-deg elbow, 1"
1.370	Male-Female adapter, 2"	1.830	Tee Flow-Branch, 1"
0.518	Tee Flow-Run, 1"	0.610	Male-Female adapter, 1"

Other hydraulic and simulation parameters such as routing models, analysis period, reporting time steps, and dynamic wave routing were also calibrated to simulate experimental conditions. A summary of these analysis parameters is detailed in Table 4.

Table 4. EPA-SWMM parameters for the simulation of experiment 1

Storage unit property	Quantity/ Value
Invert Elevation	1.5 m
Max Depth	0.7 m
Initial Depth	0.7 m
Storage Curve	Tabular (Barrel, see Table 1a, Appendix)
Conduit property	
Roughness coefficient	n = 0.009 (Manning's)
Shape	Circular
Entry/ exit losses	Varies (see Table 2a, Appendix)
Length	Varies (see Figure 2)
Max depth	Varies (see Figure 2)
Junction property	
Surcharge Depth	200 m
Invert Elevation	Varies (See Figure 3)
Simulation Options	
Routing Model	Dynamic Wave
Analysis Period	3 minutes (Exp 1 & 2); 5 minutes (Exp 3)
Reporting Step	5 seconds
Routing Step	5 minutes
Inertial terms	Keep

Results

Experimental results

In this section, results of experiments 1-3 are presented with a brief description of reservoir outflows and discharge behavior at the demand nodes, followed by hydrographs that demonstrate flows from each trial. The data points of each hydrograph represent the average flow rate per interval of time to fill an incremental volume (3.78 liters, 1 gallon) in the collection bins or trough. Hence, each flow measurement is presented at the midpoint of the time interval. The straight lines connecting each flow point are drawn to visualize the outflow hydrograph; however, these connections do not imply experimental flow measurements were recorded between data points.

After the presentation of experiment 2 is a comparison of the average discharge rates from experiments 1 and 2, both falling-head scenarios executed at different reservoir and nodal heights. Following the empirical data, EPANET 2.2.0 outputs are displayed to illustrate difficulties experienced with IWS simulation. Finally, EPA-SWMM 5.1.015 model outputs from simulations of experiments 1-3 are presented as hydrographs and compared to the averaged experimental hydrographs at each node.

Experiment 1

Results from experiment 1, a falling-head scenario, are displayed as a reservoir outflow hydrograph in Figure 12 and demand node hydrographs in Figure 13.

From the reservoir, outflow initially peaked as it rushed into the vacated distribution system before settling into a gradually decreasing rate. As the water level reached the outlet orifice, significant outflow tapered off, approximately 60 seconds after the outflow valve was opened. The outflow valve was kept open for another 40-120 seconds to observe discharge at the demand nodes.

At nodes 15, 18, and 20, discharge was characterized by an initial surge in the first 20 seconds of the trial before settling into lower, gradually decreasing flows. After approximately 60 seconds, appreciable discharge tapered off, correlating with the duration of appreciable reservoir outflow. At node 22, significant outflows lasted past 90 seconds before tapering off. Node 22 was the only node to receive appreciable discharge after 60 seconds.

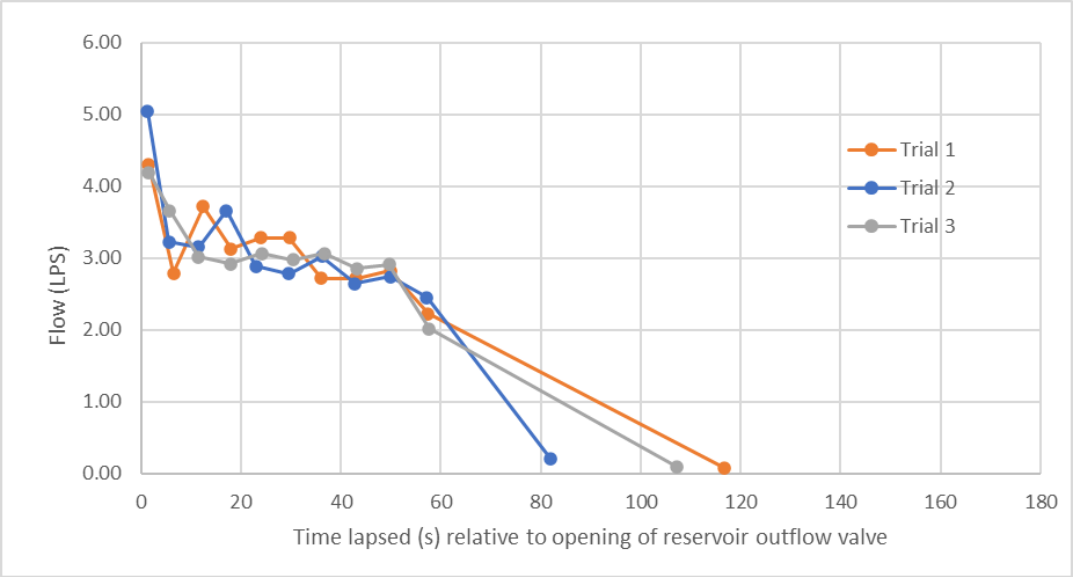

Figure 12. Reservoir outflow hydrograph for experiment 1.

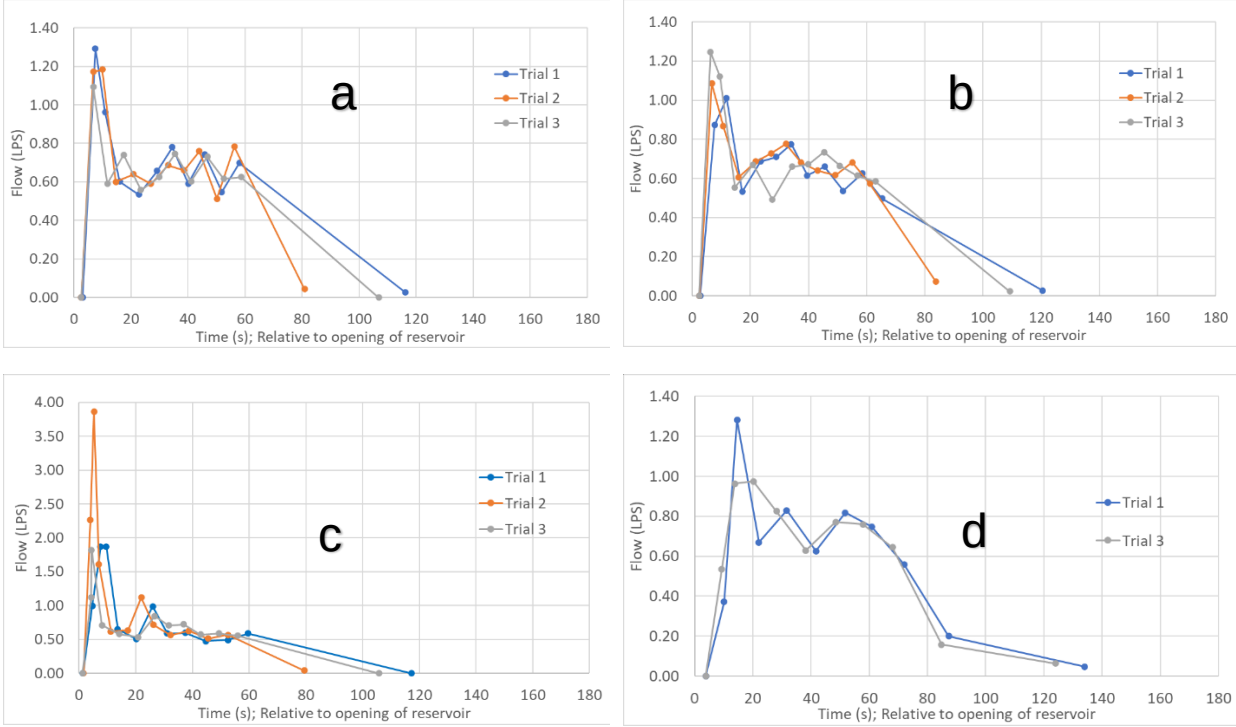

Figure 13. Demand node hydrographs for experiment 1: a) Demand Node 15 (0.6 meters), b) Demand Node 18 (0.5 meters), c) Demand Node 20 (1.0 meters). Note that scale of the y-axis, flow, reaches to 4.00 LPS, d) Demand Node 22 (0.0 meters). Trial 2 results at Node 22 were not recorded past six seconds due to a recording error by the camera.

Experiment 2

Results from Experiment 2, a falling-head scenario, are displayed as a reservoir outflow hydrograph in Figure 14 and demand node hydrographs in Figure 15.

From the reservoir, outflow initially peaked as it filled the distribution system before settling into a gradually decreasing rate. As the water level reached the outlet orifice, significant outflow tapered off, approximately 100 seconds after opening the outflow valve. The outflow valve was kept open for another 60-140 seconds to observe discharge at the demand nodes.

At nodes 15, 18, and 20, discharge was characterized by an initial surge in the first 20 seconds of the trial before settling into lower, gradually decreasing flows. At nodes 15 and 18, appreciable discharges tapered off after approximately 80-100 seconds, correlating with the duration of reservoir outflows. At node 20, the highest node (1.0 meter), appreciable discharge tapered off after approximately 60 seconds. At node 22, significant outflows lasted past 120 seconds before tapering off. Node 22, the lowest node, was the only node to receive appreciable discharge 100 seconds after the opening of the reservoir outflow valve.

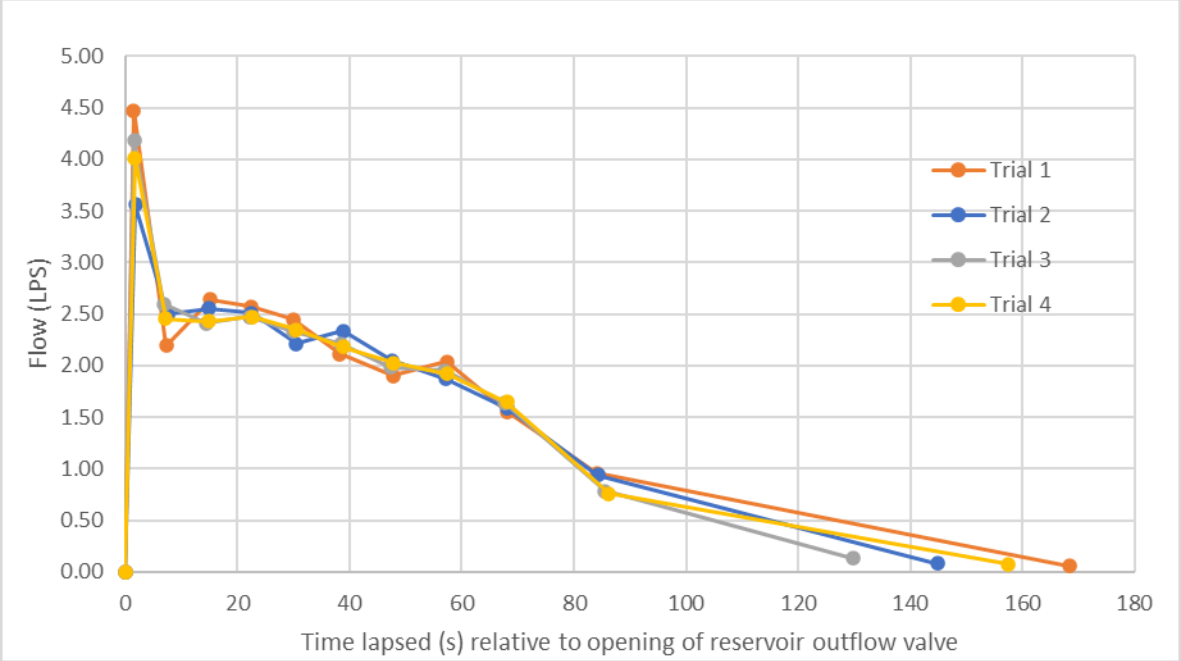

Figure 14. Reservoir outflow hydrograph for experiment 2.

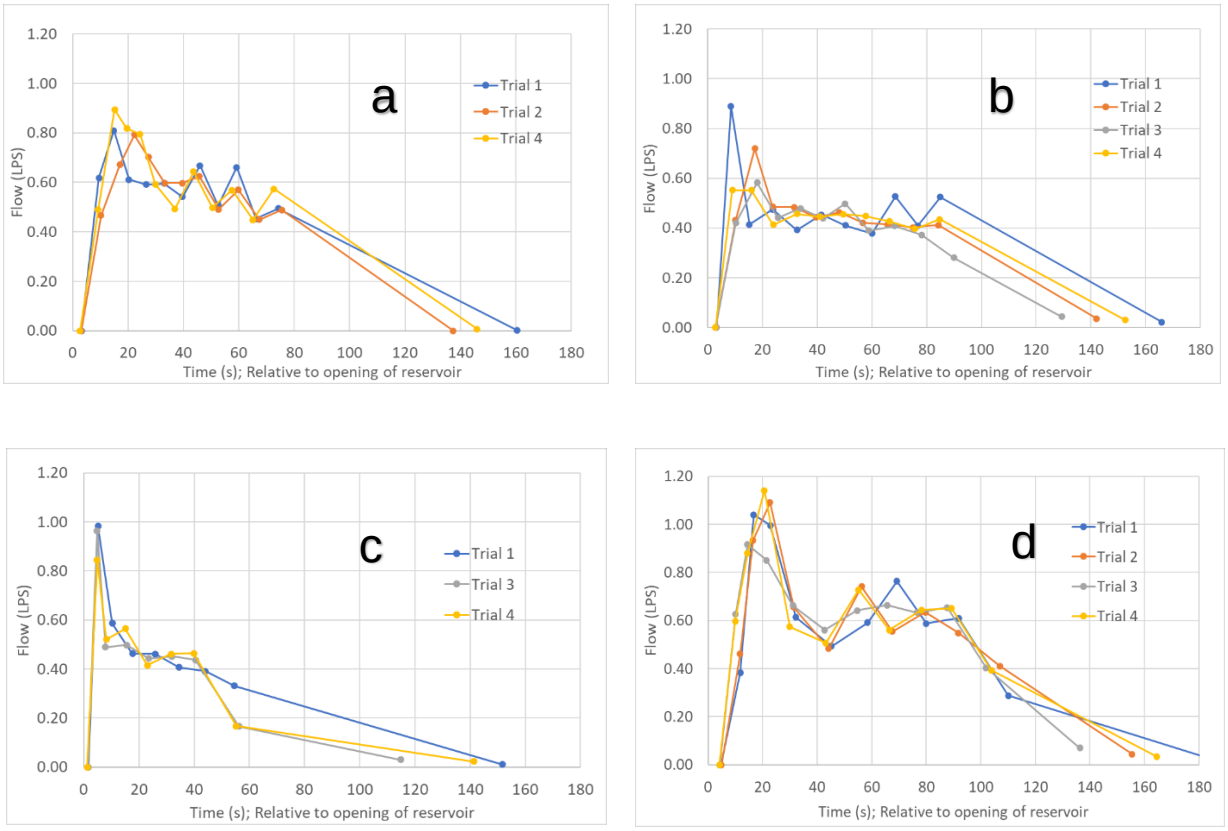

Figure 15. Demand node hydrographs for Experiment 2: a) Demand Node 15 (0.6 meters). A recording error in Trial 3 prevented data from being collected. b) Demand Node 18 (0.5 meters), c) Demand Node 20 (1.0 meters). A recording error in Trial 2 prevented a full set of data from being collected. d) Demand Node 22 (0.0 meters).

Falling-Head Comparison

The following hydrographs, Figures 16 and 17, display relationships between average discharge in the falling-head experiments, 1 and 2. At each node, the incremental fill times between gallons of discharge was averaged over the trials conducted. Again, the points imply an average flow rate per time interval and are presented at the midpoint of the interval. The incremental volume was then used to calculate the average discharge rate.

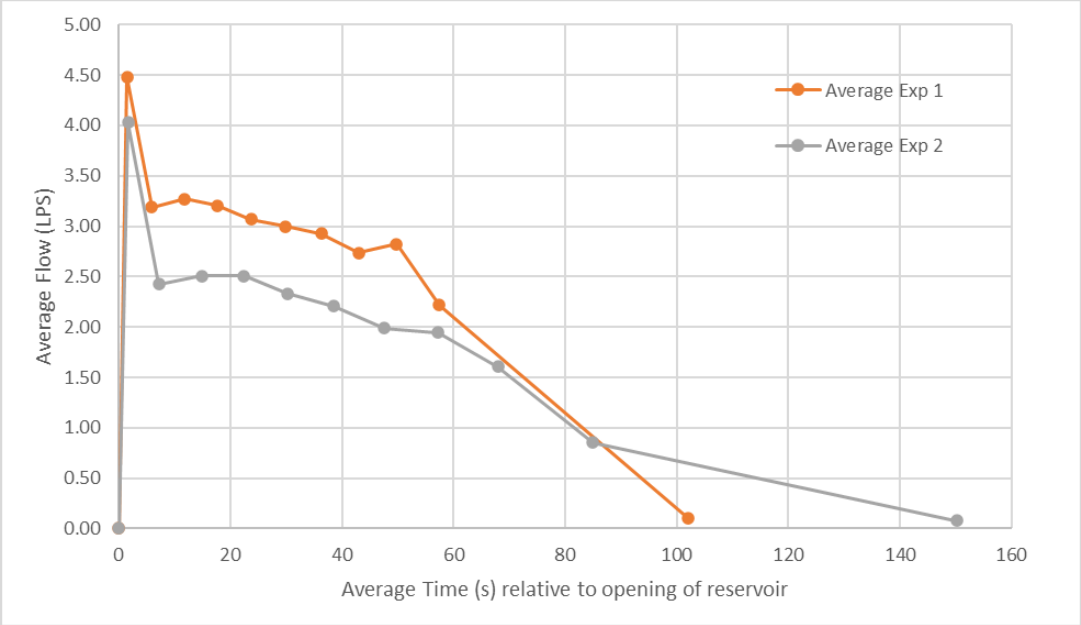

Figure 16. Average reservoir outflows measured in experiment 1 and 2.

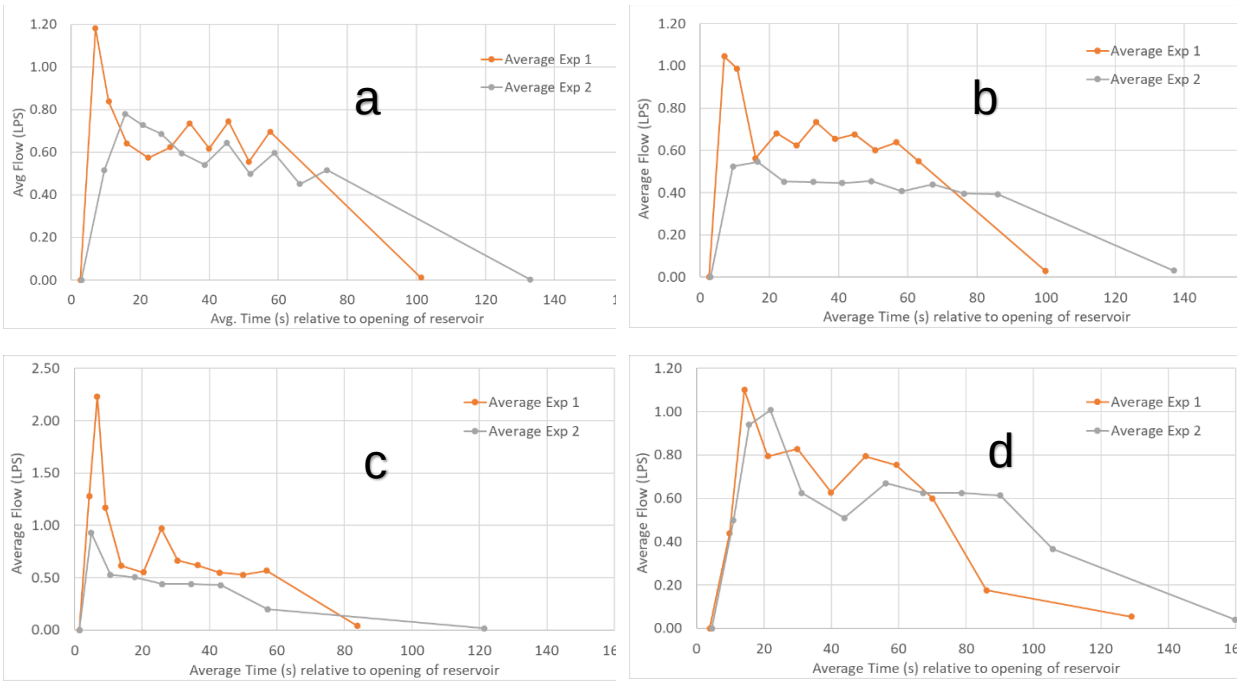

Figure 17. Average discharge measured in experiments 1 and 2: a) Demand Node 15. b) Demand Node 18, c) Demand Node 20. Note that scale of the y-axis, flow, extends to 2.50 LPS d) Demand Node 22.

Experiment 3

Results from Experiment 3, a constant-head scenario, are displayed as demand node hydrographs in Figure 18. As the level of water in the barrel was held constant, a 0.61 LPS inflow to the reservoir was matched by an estimated outflow of 0.61 LPS to the distribution system; thus, a reservoir outflow hydrograph is not included here. At nodes 15, 18, and 20, discharge was characterized by an initial trickle before building into higher, gradually increasing flows. At nodes 15 and 18, the first gallon marking was filled 100 and 80 seconds, respectively, after the opening of the reservoir valve. At node 20, the highest node (1.0 meter), a trickle of discharge occurred approximately 20-40 seconds after the opening of the reservoir valve and continued throughout each trial. Node 22, the lowest, was the only node to receive appreciable discharge throughout each trial's duration. Discharge peaked upon arrival, then settled into a constant flow rate for the remainder of the trial. In this experiment, as seen below in Figure 18, higher flows (thus, more data values) were correlated with lower demand node height.

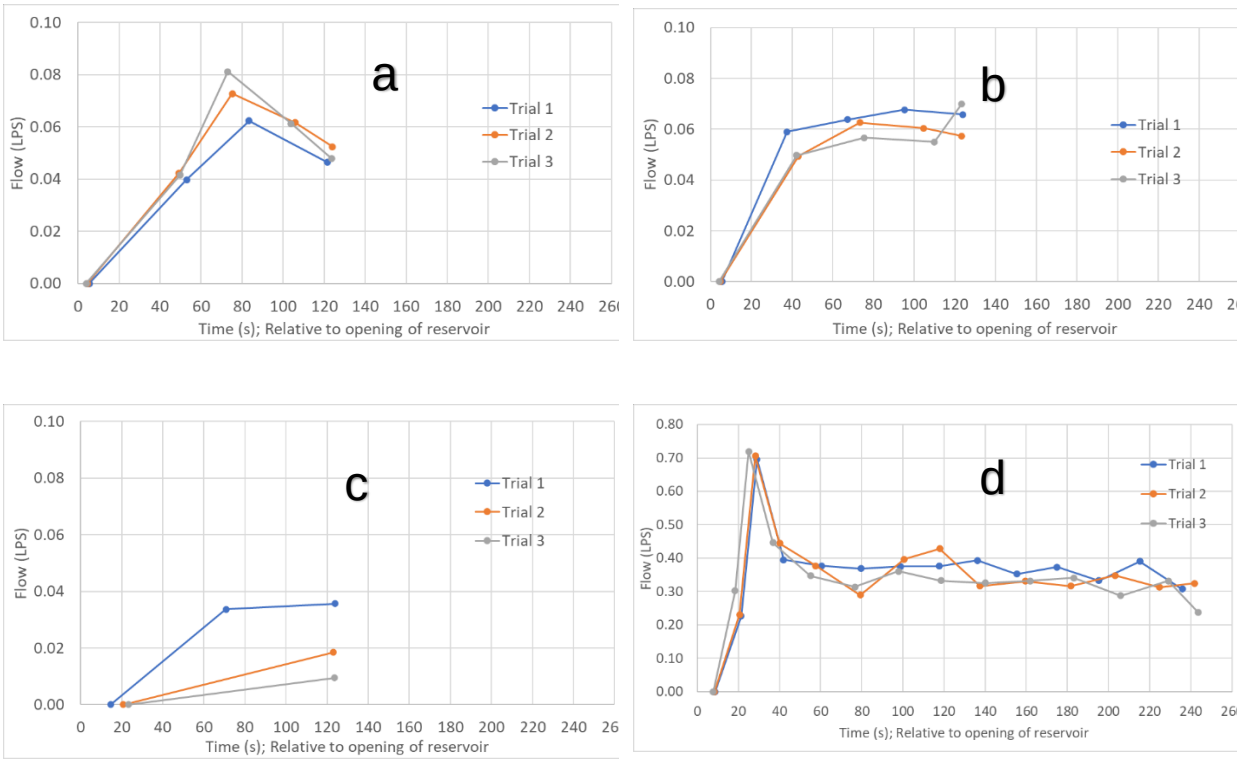

Figure 18. Demand node hydrographs for Experiment 3: a) Demand Node 15 (0.6 meters). b) Demand Node 18 (0.5 meters), c) Demand Node 20 (1.0 meters). d) Demand Node 22 (0.0 meters). Note that here, scale of the y-axis, flow, extends to 0.80 LPS.

EPANET model outputs

As seen in Figure 19, EPANET 2.2.0 was unable to replicate observed discharges or produce positive demand at all discharge nodes in experiment 1, regardless of the combination of emitter coefficients assigned (Table 2). It was determined that the program could not adequately represent the filing or emptying of network pipes under intermittent supply conditions; thus, attempts to use EPANET 2.2.0 for simulations of experiment 1, 2 and 3 were abandoned.

This phenomenon may be attributed to how the program performs hydraulic analyses. In the model, hydraulic heads and flow rates are computed simultaneously at the network's links and junctions via EPANET's Global Gradient Algorithm. This algorithm assumes pipes are constantly flowing full and computes equilibrium (steady state) flows and pressures in each time step. This balance can be seen in Figure 19, under pressure-driven demands. After the reservoir empties, EPANET nodes 17 and 12 (representing experimental nodes 22 and 18) continue to receive positive demands (outflows) while the program forces EPANET nodes 8 and 13 (representing experimental nodes 20 and 15) to report negative values of demand.

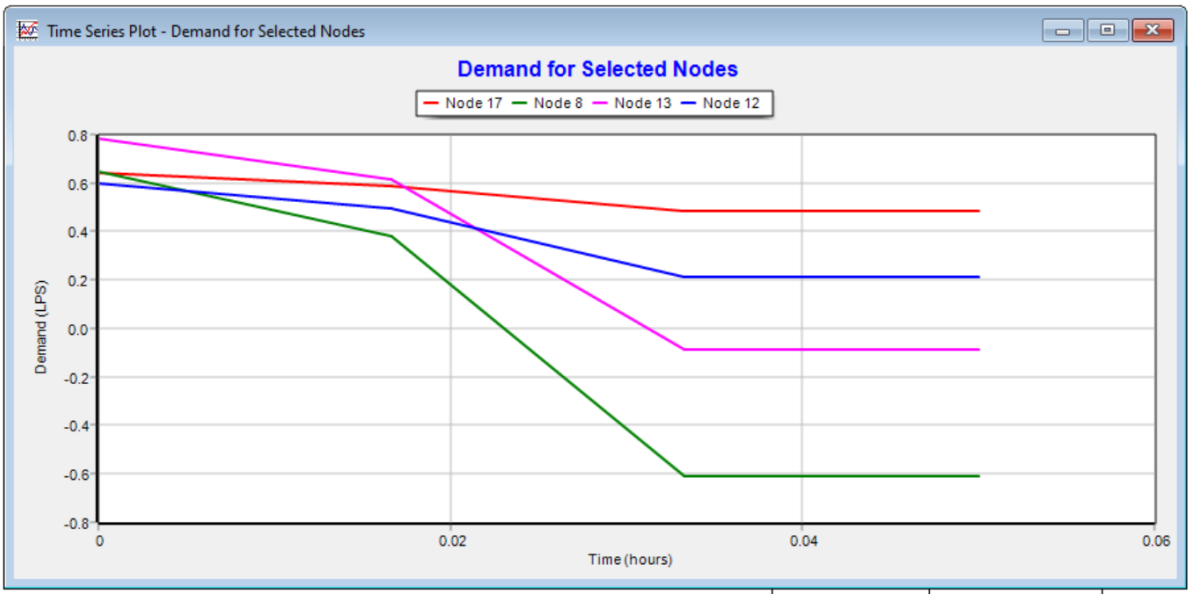

Figure 19. EPANET demand hydrographs at the four demand nodes in a simulation of Experiment 1.

EPA-SWMM model outputs and comparison to experimental results

Seen in Figure 20 are total inflow (discharge) hydrographs translated from the EPA-SWMM models of experiments 1, 2, and 3. The hydrographs generated by SWMM illustrate how the discharge pattern shape of Nodes 15, 18, and 20 are similar in each experiment. The shape of Node 22's discharge curve is also consistent across the experiments but deviates from the patterns observed at Nodes 15, 18, and 20.

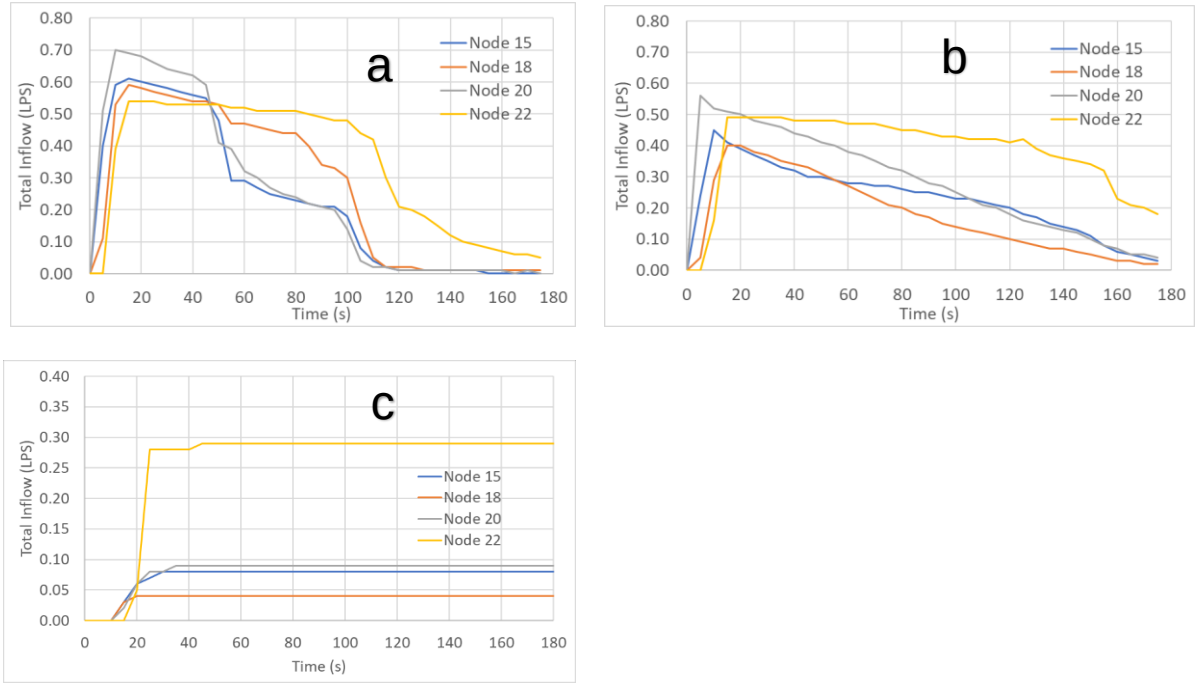

Figure 20. EPA-SWMM output hydrograph for simulations of: a) experiment 1 (falling-head). b) experiment 2 (falling-head). c) experiment 3 (constant-head). Note that here, scale of the y-axis, total inflow, extends to 0.40 LPS.

Below, Figures 21-24 show the SWMM output data in comparison to the reservoir depth graphs for experiments 1 and 2 and the average nodal hydrographs in experiments 1-3.

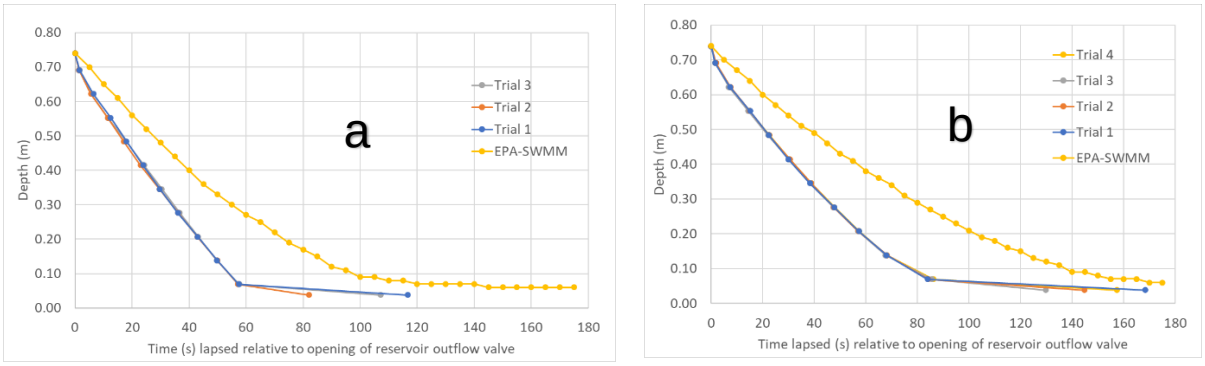

Figure 21. Experimental reservoir depths versus SWMM storage unit depths: a) experiment 1. b) experiment 2.

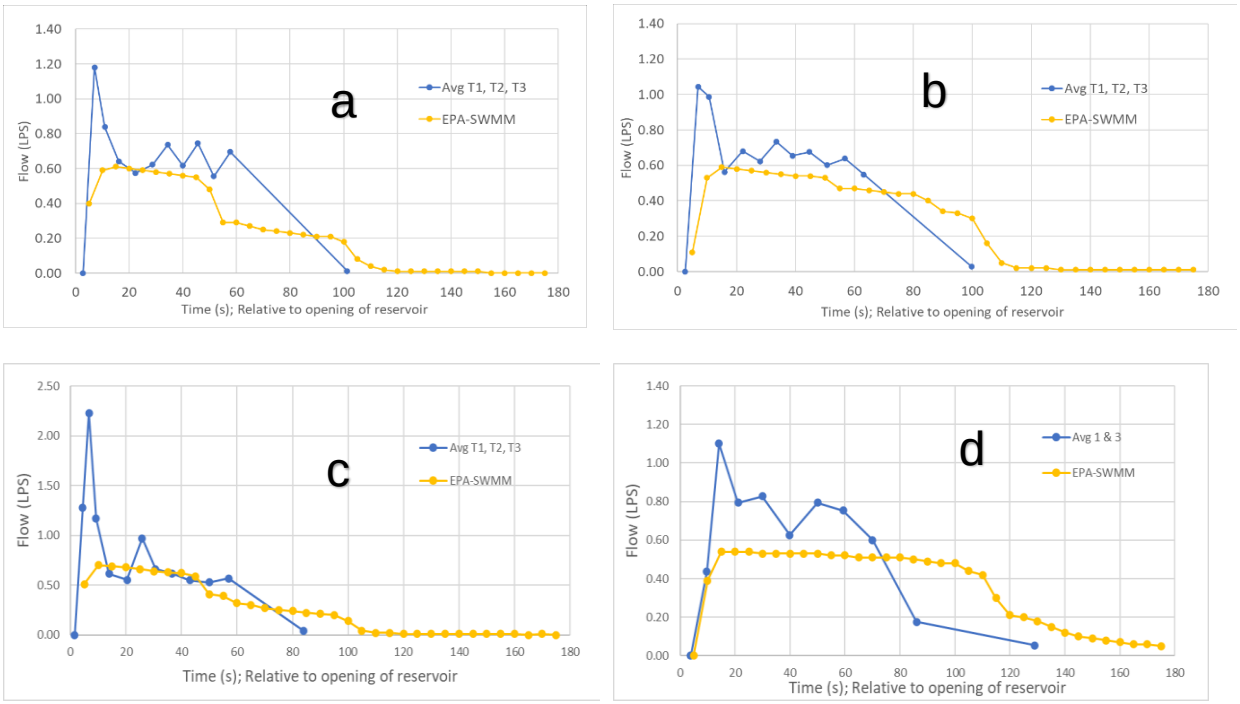

Figure 22. Average nodal hydrographs vs. EPA-SWMM model hydrographs for experiment 1: a) Demand Node 15 (0.6 meters). b) Demand Node 18 (0.5 meters), c) Demand Node 20 (1.0 meters). Note that here, scale of the y-axis, flow, extends to 2.50 LPS. d) Demand Node 22 (0.0 meters).

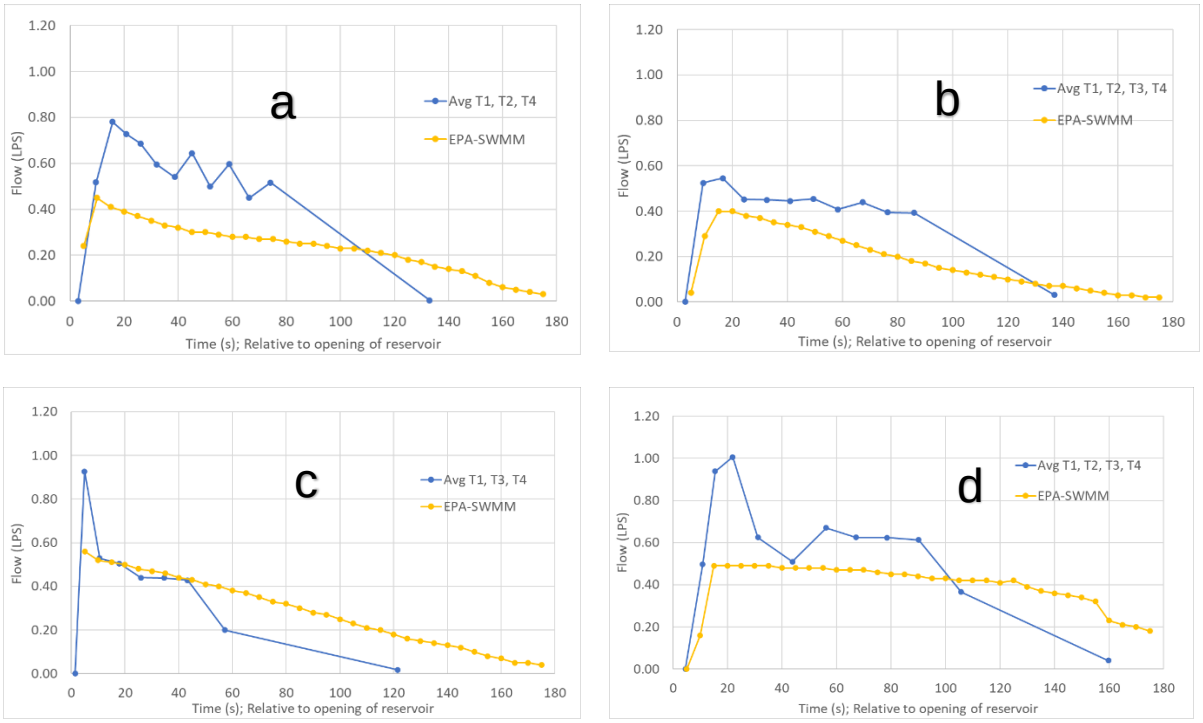

Figure 23. Average nodal hydrographs vs. EPA-SWMM model hydrographs for experiment 2: a) Demand Node 15 (0.6 meters). b) Demand Node 18 (0.5 meters), c) Demand Node 20 (1.0 meters). d) Demand Node 22 (0.0 meters).

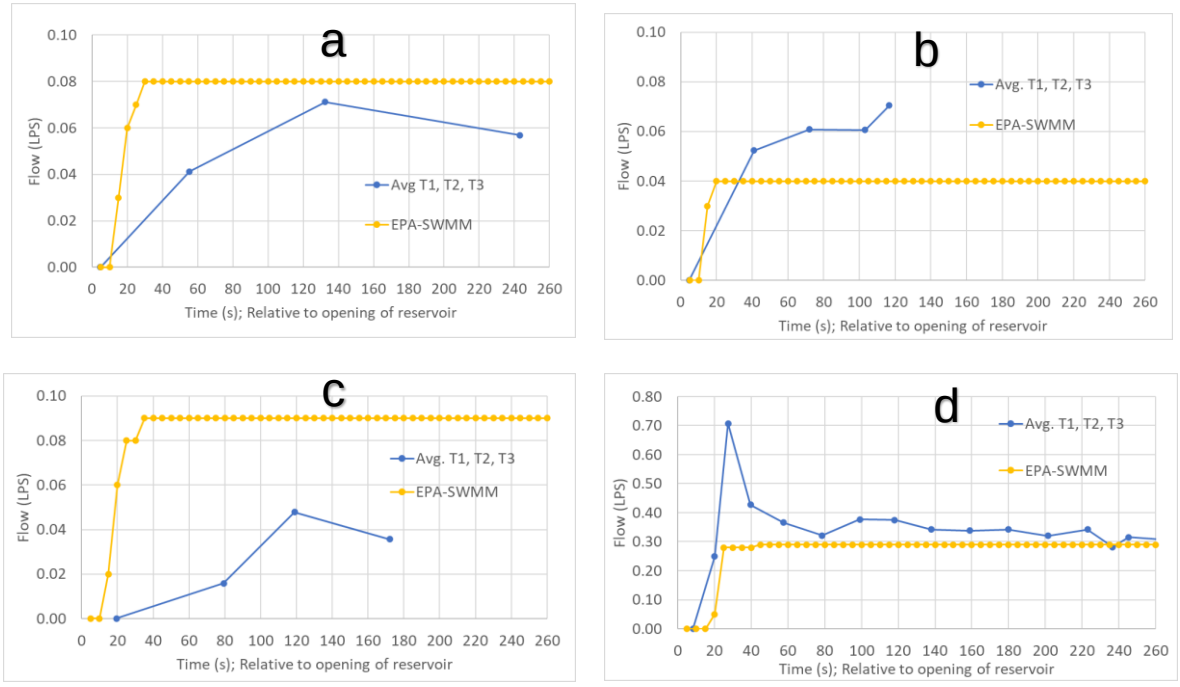

Figure 24. Average nodal hydrographs vs. EPA-SWMM model hydrographs for experiment 3: a) Demand Node 15 (0.6 meters). b) Demand Node 18 (0.5 meters), c) Demand Node 20 (1.0 meters). d) Demand Node 22 (0.0 meters). Note that here, scale of the y-axis, flow, extends to 0.80 LPS

Below, in Tables 5-7, are comparisons of average experimental discharge volumes per node versus the total inflow volumes reported by EPA-SWMM per node for each simulation. Table 8 sums these volumes and compares the experimental totals with the total simulated volumes generated by EPA-SWMM. The percent difference between experimental and modeled total volumes is calculated as well as the average percent difference in nodal volumes per experiment. Finally, losses in experimental volume are included in Table 8 and are defined as the difference between initial barrel volume (192.11 L) and the sum of the average nodal discharge volumes measured in the collection bins.

Table 5. Experiment 1 average nodal volumes vs EPA-SWMM simulation volumes. Average percent difference: 5.5%

Node	Height (m)	Exp. 1 Avg. Vol (L)	SWMM Avg. Vol (L)	Difference
15	0.6	39.43	40.4	2.5%
18	0.5	44.16	47.9	8.5%
20	1.0	42.27	44.1	4.3%
22	0.0	57.03	60.8	6.6%

Table 6. Experiment 2 average nodal volumes vs EPA-SWMM simulation volumes. Average percent difference: 9.3%

Node	Height (m)	Exp. 2 Avg. Vol (L)	SWMM Avg. Vol (L)	Difference
15	0.6	42.44	40.20	-5.3%
18	0.5	41.31	31.60	-23.5%
20	1.0	29.48	48.60	64.9%
22	0.0	67.72	68.50	1.2%

Table 7. Experiment 3 average nodal volumes vs EPA-SWMM simulation volumes. Average percent difference: 126.1%

Node	Height (m)	Exp. 3 Avg. Vol (L)	SWMM Avg. Vol (L)	Difference
15	0.6	12.62	22.40	77.5%
18	0.5	14.20	11.80	-16.9%
20	1.0	4.42	24.20	448.0%
22	0.0	82.57	79.20	-4.1%

Table 8. Comparison of total volumes generated in experiments and by EPA-SWMM simulations.

	Starting Exp. Volume (L)	Avg. Total Exp. Volume Collected (L)	Loss (L)	EPA-SWMM Total Vol. (L)	Difference in Total Vol.	Average Difference in Nodal Volumes
Experiment 1	192.11	182.89	9.22	193.20	-5.6%	5.5%
Experiment 2	192.11	180.95	11.16	188.90	-4.4%	9.3%
Experiment 3	192.11	113.80		137.60	-20.9%	126.1%

Discussion

Engineers, consultants, local, state, and federal water authorities, especially those in developing regions, could benefit from a modified, open-source water distribution modeling program that would adequately describe the discrete phases of flow (filling, pressurized, emptying) in intermittent water systems. The results of this study indicate that EPANET 2.2.0, operating under demand-driven analysis and calibrated with emitter coefficients, does not contain the computational capacity to accurately simulate discharge in transient flow conditions. Rather, EPANET 2.2.0 is better suited to fully pressurized or continuous water systems because the algorithm it employs accounts for steady flow at equilibrium. If EPANET 2.2.0 was updated with, for example, a modality to incorporate unsteady flow or dynamic wave routing similar to that employed by EPA-SWMM, the software would become accessible and accurate for managers, designers, and engineers who want to apply the software to their IWS.

Likewise, utilizing EPA-SWMM in a modified manner could, theoretically, present water managers a more accurate representation of IWS outflows. However, an appropriate application of EPA-SWMM to an IWS requires an intimate knowledge of the program's features and how to orient them in a manner that emulates the performance of water distribution infrastructure. For example, reservoirs are not modeling components of EPA-SWMM and must be substituted for "storage units" in falling-head scenarios and represented by a fixed outfall in a constant-head scenario. Therefore, an ideal update or entirely new software package could build an intermittent water distribution design suite around EPA-SWMM's underlying hydraulic modeling capabilities.

In both falling-head simulations, EPA-SWMM underestimated discharge across demand nodes (Figures 22 and 23, Table 8). The initial surge of flow observed in the falling-head trials is not captured by the models and remains a source of error between the experimental and virtual IWS. However, a surge was simulated in early versions of the EPA-SWMM model built by the researchers. As subsequent versions of the model assigned entry and exit loss coefficients to conduits, this surge disappeared. This omission may be attributed to the addition friction losses accounted for by SWMM at the ends of each conduit, as enumerated in Table 2a (Appendix).

A discrepancy in reservoir outflow rates (Figure 21) may also play a role in SWMM's inability to model flow variability observed in the experiments. EPA-SWMM modeled storage unit outflow at a steadier, slower rate than reservoir outflow observed in the experiments. In EPA-SWMM, outflow from the storage unit is determined from the conservation of mass and energy, while storage volume is described as a function of surface area (m^2) per stage (m), detailed in a tabular storage curve (Table 1a). However, experimental reservoir outflow was directed through a 2-inch ball valve; although sudden, the opening of the reservoir's outflow ball valve constitutes a transient event. This event was likely not accounted for in EPA-SWMM because the program does not model a valve transitioning from closed to open; storage unit volume is simulated as constant in one time step and emptying into a connected conduit in the next (representing a completely open valve).

Furthermore, decreases in height between nodes produce significant slopes that may serve to accelerate flow. For example, between nodes 1 and 5 (Figure 3) an elevation change of 0.4 meters occurs over the approximately 1.0-meter length of 50.8 mm (2-inch) PVC pipe, producing a slope of 40 percent. Hydrostatic pressure cannot be assumed in pipes at slopes of 10 percent or more; however, SWMM may not account for this discrepancy. This may help explain why simulated flows discharging from SWMM's distribution system could not mimic the initial discharge surges observed in the experiments.

While EPA-SWMM failed to account for these flow transients, the model simulations reproduced the general shape and duration of the empirical hydrographs. Furthermore, regarding the differences in average nodal discharge volumes and total discharge volumes calculated from experiments 1 and 2 (Table 8), EPA-SWMM generated results within 10 percent of observed discharge volumes. Thus, EPA-SWMM demonstrates an ability to predict, with some degree of accuracy, the volumes observed in the falling-head scenarios.

In the constant-head scenario of experiment 3, the model overpredicted simulated volumes at the elevated nodes (15, 18, and 20); however, SWMM predicted outflows at Node 22 within an accuracy of 5% (Table 7). In experiment 3, the trials were likely not performed long enough or with a sufficient reservoir outflow rate for the system to reach a pressurized state. Perhaps under pressurized flow, experimental discharge would approach the discharge rates predicted by SWMM.

As seen above in the outflow hydrographs and volume tables of each demand node, a correlation exists between the height of the discharge point and the quantity of water received. This phenomenon is repeated in both the EPA-SWMM model and in the literature reviewed above (Dubasik, 2016). Thus, according to Bernoulli's equation, it should be expected that Node 22, discharging at the level of the floor into the trough consistently received the highest discharge volume.

Study Limitations

Error in discharge measurements existed in the first experiment as the research team relied on cameras and a stopwatch to capture the translucent water in translucent bins. Thus, it was recognized that a higher resolution recording equipment and tinted water could improve the accuracy of the measurements. Blue food dye was added to the water in experiments 2 and 3 to facilitate clearer observation of discharge volumes in the collection bins and the reservoir. In experiments 1 and 2, the research team experienced recording errors due to the camera running out of space on its memory card. This resulted in a fourth trial begin performed in experiment 2 to gather three sets of data at all demand nodes. Future experiments should employ higher capacity memory cards or empty the cards at the end of the experiment.

Despite the enhanced visibility of tinted water, the discharge recorded in the bins, especially at the beginning of each trial, was subject to imprecision. Primarily, when water surged out of the demand node and splashed into the underlying bin, the level of water corresponding to an

incremental gallon (3.78 liters) volume was difficult to assess. As the bin filled, the procession of water level between gallon increments, noted on the side of the bin in permanent marker, was more easily observed because the splashing effect had dampened.

When the collected discharge rose between gallon increments, the time was recorded to calculate the incremental discharge rate. However, due to the resolution of the cameras and possible error in the location of gallon marks on the bin, the true time for discharge to fill a gallon is subject to error. Furthermore, difficulty experienced when reading water levels may indicate that recorded discharge varies by a volume corresponding to the thickness of the gallon markings (approximately 0.44 liters). Total volume measurements were also subject to error because markings were annotated as whole gallons and discharge levels read between markings were estimated based on the proximity to the upper or lower marking.

Losses of water that occurred between the reservoir and the collection bins produce another form of experimental error. Table 8 details that 9.22 liters were unaccounted for in experiment 1, and 11.16 liters were lost in experiment 2. Losses were not calculated for experiment 3, as the reservoir's volume was held constant and a precise reservoir outflow rate was not known because water was observed passing through the overflow orifice. One explanation for the discrepancies in volume is a leak discovered in Node 22's collection device, a drainage trough in the floor of the laboratory. Losses also occurred from a loose fitting at node 1 and from splashing at each collection bin when discharge initially surged from the demand nodes. Finally, residual water was discovered within the system, near the junctions, after completion of the trials.

The relatively short length of the experiments, as well as the relatively low volume of water used to fill the system, may have limited the laboratory system's ability to reach a pressurized state. Flow meters or translucent piping may have allowed researchers to observe network water levels in real-time to validate whether the pipes ever reached a full or pressurized state. Thus, it is inferred that many of the pipes included in this study are operating first in the "filling" stage followed by an "emptying" stage.

Experiment 3, the constant-head scenario, may include a discrepancy between the inflow and outflow rates at the reservoir. The inflow rate received from a hose attached to the laboratory's municipal tap was determined to be approximately 0.61 LPS. The outflow rate from the reservoir, with the outflow valve completely open and starting with 1.7 meters of head was determined to be approximately 2.60 LPS. Therefore, an intermediate position or rotation of the ball valve was identified to accommodate the inflow. However, in the trials, rotating the valve's handle to this precise location proved difficult. Therefore, while an outflow of 0.61 LPS is assumed to enter the distribution network in experiment 3, the true reservoir outflow may have ranged above and below that assumed figure, depending on the position of the valve.

The particular dimensions of the laboratory-scale IWS also limits the interpretation and generalizability of the study results. The ratios of PVC pipe -diameters and lengths -to the -reservoir -size does not accurately reflect the scale associated with actual IWS systems. While

the pipes utilized in the experimental system represent commercially available sizes common in distribution networks, the lengths of the pipes, the size of the storage reservoir, and the changes in elevation are not to scale. For example, the 2-inch PVC piping connected to the 50.75-gallon barrel may also be appropriate to drain larger, community-sized reservoirs. Thus, if the laboratory's barrel is expected to simulate larger storage structures, the size of the distribution piping should decrease to better simulate an actual distribution network. Junction and valve sizes may also be better approximated at smaller sizes. Furthermore, other characteristics of the experimental system, such as the slope, length, or layout of conduit, may not be representative of larger IWS built in many developing regions of the world.

Incongruencies between measured and modeled flow may be attributed to complexities presented in the construction of the laboratory-scale IWS. For example, at junctions where pipe diameter decreased between conduits, adapters were installed immediately up- or downstream of the junction because the reduction in diameter was not possible in the single-size fittings utilized. This combination of flow obstructions in-series, as well as a complex flow pattern, would likely augment the energy losses experienced at the node. However, when identifying entry/ exit coefficients at each conduit in EPA-SWMM, only a single coefficient relating to the fitting type, was identified. A similar situation is experienced with modeling the losses associated with rubber radiator hose fittings that permitted sharp declines between junctions. Future analyses of this system could account for multiple losses in a flow path by estimating a composite loss coefficient, “Keq.” The composite loss coefficient would represent the sum of individual losses experienced at the entry or exit points of a pipe.

Conclusions

This report aimed to examine the hydraulic performance of IWS and the abilities of open-source water distribution and stormwater conveyance software programs to accurately represent that performance. The three experiments performed on a laboratory-scale IWS simulated two scenarios: falling-head and constant-head, which are common pressure schemes experienced by actual IWS. The data produced from each of these experiments illustrated how gravity-fed discharge is distributed among four demand nodes, or points of use, at varying elevations. Results from the experiments indicate that the highest flows tended to be distributed to the lowest demand nodes, as Node 22 which discharged at the level of the floor consistently received the highest discharge volumes.

Two virtual water distribution networks were constructed in EPANET 2.2.0 and EPA-SWMM 5.1.015 to mimic the laboratory-scale IWS. EPANET was calibrated using emitter coefficients and constructed with typical water distribution components. However, analysis of the demand node discharge revealed EPANET to be inadequate in representing transient flow conditions, so simulation of the falling-head and constant-head experiments was abandoned. However, SWMM, manipulated to mimic the momentum of unsteady flow in gravity-fed IWS, produced plausible results for each experiment. Total discharge volumes generated in SWMM were compared to the total discharge volumes measured in the experiments (Table 8). SWMM was

discovered to overpredict total discharge volumes by 5.6% in experiment 1, 4.4% in experiment 2, and 20.9% in experiment 3. While EPA-SWMM was unable to simulate precise discharge volumes and patterns observed in the laboratory-scale IWS, it is recommended that further verification be undertaken to validate SWMM's capacity to model IWS systems under a range of hydraulic scenarios. In future modelling of IWS systems, it is also recommended that researchers account for the fluid mechanics associated with valve components that regulate flow from storage devices into the distribution network. If SWMM can approximate IWS componentry such as valves and withstand rigorous experimentation, potential may exist for this software to be extended for the design of IWS.

As this project was conducted on a tight budget and noting how many IWS systems are constructed in areas with few financial resources, low-cost solutions to improve measurement accuracy should be explored. This could take the form of a precisely metered discharge container featuring incremental markings to the tenth of a gallon (0.378 liters), as this study only marked bins per full gallon. Future projects could also measure flow and detail system parameters in metric units to avoid conversion errors. The most accurate form of flow measurement would come from electronic in-line flow meters, connected to data acquisition software and hardware. For budgetary constraints, this technology was omitted from the experiments. However, if digital metering were applied, reservoir and demand node outflows could be recorded with a higher degree of accuracy and eliminate the time and effort used to set up cameras, upload video files, watch and time the videos, input the data, and create hydrographs in Microsoft Excel. If cost is no object, an alternative form of improving the discharge accuracy could be to place scales underneath the collection bins. This way, measurement of the discharge is not dependent on cameras or gallon markings noted in a specific location on the laboratory's floor. For pressure and flow timing measurements, clear PVC sections spliced into the network near network junctions may permit real-time flow observation, which could provide a better understanding of the transient flow phases. Implementing an array of clear PVC splices may also present an opportunity to install flow or pressure sensors throughout the distribution system.

Different hydraulic scenarios could be performed on this scale-IWS system. For example, in either a falling- or constant-head scenario, a demand node's valve could be closed once a predetermined volume is achieved in the node's corresponding collection device. Closing discharge valves during operation would divert water to the remaining open nodes and demonstrate how IWS function when demands alter. Other experiments could allow a constant-head scenario to proceed much longer; the relatively low outflow and short duration of experiment 3 likely did not allow the network pipes to fill and simulate pressurized flow. If a longer constant-head experiment is pursued, larger collection devices would be required, and a higher inflow of water should be used.

References

Babonneau, F., G. Corcos, L. Drouet, and J.-P. Vial. 2019. “NeatWork: A Tool for the Design of Gravity-Driven Water Distribution Systems for Poor Rural Communities.” *INFORMS Journal on Applied Analytics*, 49 (2): 129–136. https://doi.org/10.1287/inte.2018.0983.

Cabrera-Béjar, J. A., and V. Gueorguiev Tzatchkov. 2012. “Modelación de redes de distribución de agua con suministro intermitente.” *Tecnología y ciencias del agua*, 3 (2): 05–25. Instituto Mexicano de Tecnología del Agua, Coordinación de Comunicación, Participación e Información.

Campisano, A., A. Gullotta, and C. Modica. 2018. “Using EPA-SWMM to simulate intermittent water distribution systems.” *Urban Water Journal*, 15 (10): 925–933. Taylor & Francis Ltd. https://doi.org/10.1080/1573062X.2019.1597379.

Dubasik, F. 2017. “PLANNING FOR INTERMITTENT WATER SUPPLY IN SMALL GRAVITY-FED DISTRIBUTION SYSTEMS: CASE STUDY IN RURAL PANAMA.” *Dissertations, Master’s Theses and Master’s Reports*. https://doi.org/10.37099/mtu.dc.etdr/498.

Engineering ToolBox, (2004)a. *Manning's Roughness Coefficients*. [online] Available at: https://www.engineeringtoolbox.com/mannings-roughness-d_799.html [Accessed Day Mo. Year].\

Engineering ToolBox, (2004)b. *Pipe and Tube System Components - Minor (Dynamic) Loss Coefficients*. [online] Available at: https://www.engineeringtoolbox.com/minor-loss-coefficients-pipes-d_626.html [Accessed Day Mo. Year

Engineering ToolBox, (2004)c. *PVC Pipes - Equivalent Length and Pressure Loss in Fittings*. [online] Available at: https://www.engineeringtoolbox.com/pvc-pipes-equivalent-length-fittings-d_801.html [Accessed Day Mo. Year].

Kumpel, E., and K. L. Nelson. 2016. “Intermittent Water Supply: Prevalence, Practice, and Microbial Water Quality.” *Environ. Sci. Technol.*, 50 (2): 542–553. American Chemical Society. https://doi.org/10.1021/acs.est.5b03973.

McKenzie, F. 2011. “Study of water use and supply in the district of Independencia, Peru.” *Dissertations, Master’s Theses and Master’s Reports - Open*. https://doi.org/10.37099/mtu.dc.etds/519.

Mihelcic, J. R., Phillips, L.D., Fry, L.M., Barkdoll, B.D., Myre, E.A. 2009. *Field guide to environmental engineering for development workers: water, sanitation, and indoor air*. Reston, Va: American Society of Civil Engineers.

Rossman, L., H. Woo, M. Tryby, F. Shang, R. Janke, AND T. Haxton. EPANET 2.2 User Manual. U.S. Environmental Protection Agency, Washington, DC, EPA/600/R-20/133, 2020.

Rossman, L. Storm Water Management Model Reference Manual Volume II – Hydraulics. U.S. Environmental Protection Agency, Washington, DC, EPA/600/R-17/111, 2017.

Appendix

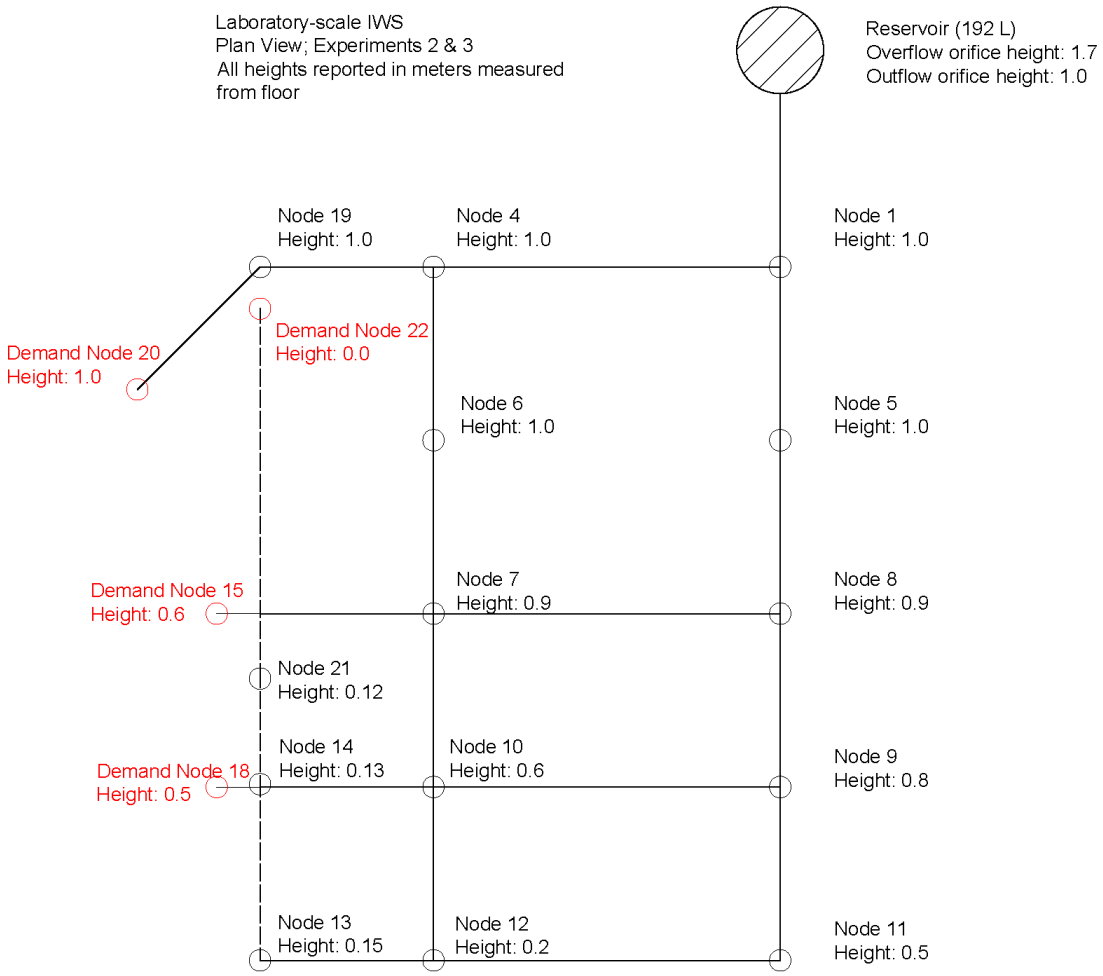

Figure 1a. Node height map for experiments 2 and 3

Table 1a. EPA-SWMM tabular storage curve for storage unit (experiments 1 and 2

Stage in storage unit	Surface Area
0.0	0.2739
0.1	0.2739
0.2	0.2739
0.3	0.2739
0.4	0.2739
0.5	0.2739
0.6	0.2739
0.7	0.2739

Table 2a. EPA-SWMM conduit entry and exit loss coefficients

Conduit	Entry	Description	Exit	Description
1	k = 0.05/ 200	Ball valve, 2"/	1.310	Tee Flow-Run, 2"
2	1.310	Tee Flow-Run, 2"	1.370	Male-Female adapter, 2"
3	1.370	Male-Female adapter, 2"	0.518	Tee Flow-Run, 1"
4	0.518	Tee Flow-Run, 1"	0.518	Tee Flow-Run, 1"
5	0.518	Tee Flow-Run, 1"	1.620	90-deg elbow, standard sharp inside radius, 1"
6	1.310	Tee Flow-Run, 2"	2.440	Tee Flow-Branch, 1.5"
7	0.427	45-deg elbow, 1"	0.427	45-deg elbow, 1"
8	0.518	Tee Flow-Run, 1"	1.830	Tee Flow-Branch, 1"
9	0.518	Tee Flow-Run, 1"	1.830	Tee Flow-Branch, 1"
10	1.620	90-deg elbow, standard sharp inside radius, 1"	1.830	Tee Flow-Branch, 1"
11	1.830	Tee Flow-Branch, 1"	k = 0.04	Coupling, 1"
12	k = 0.04	Coupling, 1"	1.830	Tee Flow Branch, 1"
13	1.830	Tee Flow-Branch, 1"	1.830	Tee Flow-Branch, 1"
14	1.830	Tee Flow-Branch, 1"	1.830	Tee Flow-Branch, 1"
15	1.830	Tee Flow-Branch, 1"	0.427	45-deg elbow, 1"
17	1.830	Tee Flow-Branch, 1"	1.620	90-deg elbow, standard sharp inside radius, 1"
18	1.620	90-deg elbow, standard sharp inside radius, 1"	k = 0.04	Coupling, 1"
19	k = 0.04	Coupling, 1"	k = 0.04	Coupling, 1"
21	1.830	Tee Flow-Branch, 1"	0.427	45-deg elbow, 1"
22	1.830	Tee Flow-Branch, 1"	0.427	45-deg elbow, 1"
23	k = 0.04	Coupling, 1"	0.427	45-deg elbow, 1"